Available online at www.sciencedirect.com
ScienceDirect
Deep-Sea Research I 54 (2007) 747–773
DEEP-SEA RESEARCH PART I
www.elsevier.com/locate/dsri

Primary productivity, differential size fraction and pigment composition responses in two Southern Ocean in situ iron enrichments

V.P. Lance[a,*], M.R. Hiscock[a,1], A.K. Hilting[a,2], D.A. Stuebe[a,3], R.R. Bidigare[b], W.O. Smith Jr.[c], R.T. Barber[a]

[a]*Nicholas School of the Environment and Earth Sciences, Duke University, 135 Duke Marine Lab Road, Beaufort, NC 28516, USA*
[b]*Department of Oceanography, University of Hawaii at Manoa, 1000 Pope Road, Honolulu, HI 96822, USA*
[c]*Virginia Institute of Marine Science, College of William and Mary, Gloucester Point, VA 23062, USA*

Received 3 June 2006; received in revised form 22 February 2007; accepted 25 February 2007
Available online 12 March 2007

Abstract

Two in situ iron-enrichment experiments were conducted in the Pacific sector of the Southern Ocean during summer 2002 (SOFeX). The "north patch," established within the Subantarctic Zone (~56°S), was characterized by high nitrate (~21 mmol m^{-3}) but low silicic acid (2 mmol m^{-3}) concentrations. North patch iron enrichment increased chlorophyll (Chl) by 12-fold to 2.1 mg m^{-3} and primary productivity (PP_{EU}) by 8-fold to 188 mmol C m^{-2} d^{-1}. Surprisingly, despite low silicic acid concentrations, diagnostic pigment and size-fraction composition changes indicated an assemblage shift from prymnesiophytes toward diatoms. The "south patch," poleward of the Southern Boundary of the Antarctic Circumpolar Current (SBACC) (~66°S), had high concentrations of nitrate (~27 mmol m^{-3}) and silicic acid (64 mmol m^{-3}). South patch iron enrichment increased Chl by 9-fold to 3.8 mg m^{-3} and PP_{EU} 5-fold to 161 mmol C m^{-2} d^{-1} but, notably, did not alter the phytoplankton assemblage from the initial composition of ~50% diatoms. South patch iron addition also reduced total particulate organic carbon:Chl from ~300 to 100; enhanced the presence of novel non-photosynthetic, but fluorescent, compounds; and counteracted a decrease in photosynthetic performance as photoperiod decreased. These experiments show unambiguously that in the contemporary, high nitrate Southern Ocean increasing iron supply increases primary productivity, confirming the initial premise of the Martin Iron Hypothesis. However, despite a 5-fold increase in PP_{EU} under iron-replete conditions in late summer, the effect of iron on annual productivity in the Southern Ocean poleward of the SBACC is limited by seasonal ice coverage and the dark of polar winter.

Keywords: Primary production; Chlorophylls; Phytoplankton; Iron; Photosynthetic pigments; Carotenoids; Photoperiod; Southern Ocean; SOFeX

*Corresponding author. Tel.: +1 252 504 7631.
E-mail address: vplance@duke.edu (V.P. Lance).
[1]Program in Atmospheric and Oceanic Sciences, Princeton University, Princeton, NJ 08544, USA.
[2]National Ocean Service, Beaufort Laboratory, Beaufort, NC 28516, USA.
[3]School of Marine Science and Technology, University of Massachusetts-Dartmouth, New Bedford, MA 02744, USA.

0967-0637/$ - see front matter © 2007 Elsevier Ltd. All rights reserved.
doi:10.1016/j.dsr.2007.02.008

1. Introduction

Advocates of its importance in climate dynamics claim the Southern Ocean has a large impact on the global carbon cycle due to its size, its reservoir of macronutrients and its role in deep water formation and re-distribution (Sigman and Boyle, 2000; Sarmiento et al., 2004). Martin's (1990) Iron Hypothesis postulated that during dry, dusty glacial periods an increase in atmospheric deposition of iron into the high nutrient waters of the Southern Ocean would increase primary productivity and increase particulate carbon flux into the deep ocean, ultimately resulting in the redistribution of atmospheric carbon dioxide into the deep ocean carbon reservoir. A decade of bottle experiments and mesoscale in situ iron-enrichment experiments in a variety of high nutrient, low chlorophyll (HNLC) waters has now conclusively demonstrated that iron addition does indeed increase primary productivity in HNLC waters (de Baar et al., 2005; Boyd et al., 2007).

Diatoms, which have been thought to play a particularly significant role in the export of carbon to the deep sea (Smetacek, 1985; Dugdale et al., 1995) and therefore are expected to be involved in maintaining the inorganic carbon gradient between the surface mixed layer and deep water, have an absolute requirement for silicic acid. In bottle experiments using natural phytoplankton assemblages, interactions between iron and silicic acid uptake have been demonstrated repeatedly (Takeda, 1998; Hutchins et al., 2001; Franck et al., 2003). Understanding in situ interactions of silicic acid availability with iron availability in relation to primary productivity and subsequent carbon partitioning, then, is integral to understanding and quantifying carbon processes, particularly in the Southern Ocean where the extreme range of imbalanced Si:N ratios (anomalously low in the Subantarctic Zone and anomalously high poleward of the Southern Boundary of the Antarctic Circumpolar Current (SBACC)) in euphotic, surface waters may have global biogeochemical implications (Sarmiento et al., 2004).

Prior to the 2002 Southern Ocean Iron Experiment (SOFeX) experiments reported here, two in situ iron-enrichment experiments had been conducted in the HNLC Southern Ocean. The Southern Ocean Iron-Enrichment Experiment (SOIREE) took place during late austral summer (February 1999) in the Pacific Sector just poleward of the Antarctic Polar Front and equatorward of the Southern Antarctic Circumpolar Current Front where silicic acid concentrations were $\sim$10 mmol m^{-3} (Boyd et al., 2000). The Eisen Experiment (EisenEx) was carried out in the Antarctic Polar Front Zone of the Atlantic Sector in austral spring (November 2000) at a time and place where the silicic acid concentration again was $\sim$10 mmol m^{-3} (Gervais et al., 2002). Both of these iron addition experiments resulted in increases in chlorophyll (Chl) biomass and primary productivity and some shift in the relative composition of the phytoplankton assemblage over the course of their 13-d (SOIREE) and 22-d (EisenEx) durations.

Both SOIREE and EisenEx were conducted within a narrow band of the Southern Ocean between the Subantarctic Zone and SBACC where nitrate remains above limiting concentrations ($\sim$20–25 mmol m^{-3}) (Boyd et al., 2000; Gervais et al., 2002), but where a seasonally transitional, steep silicon gradient exists (Nelson et al., 2001; Hiscock et al., 2003). In distinction from these earlier experiments, the SOFeX experiments were conducted in the Subantarctic Zone with perpetually low silicic acid ($\sim$2 mmol m^{-3}) concentrations (''north patch'' experiment) and in the region poleward of the SBACC with perpetually high silicic acid ($\sim$60 mmol m^{-3}) concentrations (''south patch'' experiment) (Coale et al., 2004). Here we define low concentrations of nutrients as those concentrations in the linear portion of the Michaelis–Menton-like uptake hyperbola and high concentrations as those that are saturating but not inhibiting uptake. Nelson et al. (2001) saw the onset of Si uptake limitation at about 8–10 mmol m^{-3} silicic acid for most regions of the Southern Ocean, although limitation values poleward of the SBACC were much higher ($\sim$40–50 mmol m^{-3} silicic acid). Together, the Subantarctic Zone plus the seasonally ice covered zone poleward of the SBACC make up approximately 80% of the circumpolar Southern Ocean (from Table 2 in Moore et al., 2000). SOFeX was designed to test the proximate role of iron availability in Martin's Iron Hypothesis in regulating primary production, community structure and carbon export in these two disparate, but widespread and perhaps globally significant Southern Ocean biogeochemical environments.

In this study, we quantify the responses of phytoplankton production to iron addition in two distinct regions of the Southern Ocean and interpret those responses with respect to distinguishing

between the effect of iron addition on phytoplankton physiology and phytoplankton assemblage in the water column. Specifically, we show that, despite low silicic acid concentration, the Subantarctic Zone (56°S) responded to iron enrichment with a dramatic shift to a diatom-dominated assemblage in a qualitatively similar manner to previous iron addition experiments in the Southern Ocean and elsewhere (de Baar et al., 2005; Barber and Hiscock, 2006). That is, absolute Chl concentrations and primary productivity increased in all phytoplankton size fractions and functional groups (as indicated by photosynthetic pigments), but the proportional dominance of Chl biomass and primary production shifted from small non-diatoms to large diatoms. The new information in this experiment is that the waters poleward of the SBACC (66°S) responded to iron enrichment in a fundamentally different way from the responses in all other iron-enrichment experiments to date. That is,

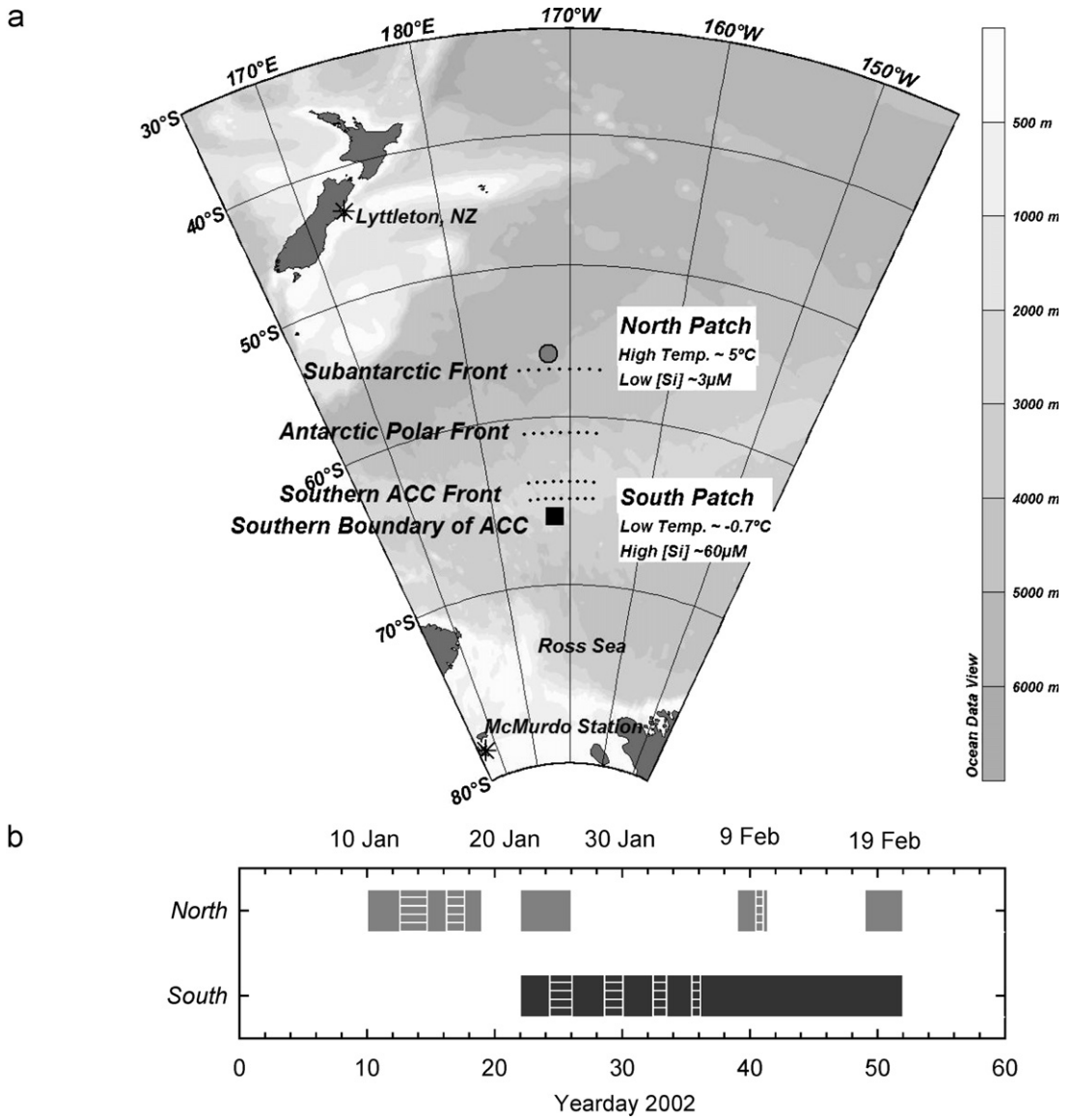

Fig. 1. (a) Map of experimental north and south patch locations. Dotted lines indicate latitudinal positions where the major fronts and boundaries cross 172°W longitude (Orsi et al., 1995). Shading indicates bathymetry (Schlitzer, 2003). (b) Activity timeline for both experimental patches. Hatch marks represent time periods of iron fertilization.

while absolute Chl concentrations and primary productivity increased several-fold in all size fractions and functional groups, *the proportional distribution of Chl concentrations and primary production remained relatively unaffected by iron enrichment poleward of the SBACC.*

2. Methods

2.1. Experimental design

The SOFeX experimental design exploited the sharp silicon gradient of the Southern Ocean to test the productivity response to iron enrichment in both high and low silicic acid regions of HNLC waters and is explained in Coale et al. (2004) but reviewed here briefly to provide context. Iron was added to two sites, both characterized by year-round high nitrate concentrations, at two latitudes in the Pacific Sector of the Southern Ocean along longitude 172°W (Fig. 1a) during mid- to late austral summer (January–February 2002). Acidified iron sulfate mixed with seawater was released at a depth of about 5 m aft of the ship's propellers. Sulfur hexafluoride (SF_6), an inert tracer gas, accompanied the initial iron infusion at each patch (Wanninkhof et al., 2004). Initial patches of approximately 15 km × 15 km were established in a period of about 2 d by releasing iron and SF_6 as the ship traversed parallel tracks in a Lagrangian grid (Coale et al., 2004). The north patch site (56°S, 172°W), equatorward of the Antarctic Frontal Zone and within the Subantarctic Zone where year-round silicic acid concentration is low, was initially fertilized on 12 January 2002, re-fertilized 1 week later and then fertilized a third time 1 month later. Total elapsed time from the day of initial enrichment to final observation was 40 d (Fig. 1b). The south patch site was located poleward of the SBACC at 66°S where year-round silicic acid concentration is high. The south patch was initially fertilized on 24 January 2002 and re-fertilized three additional times over the subsequent 2-week period. The south patch was monitored continuously for a period of 23 d with additional observations in mid-February from patch days 21 to 27, giving a total elapsed coverage from day of first enrichment of 27 d (Fig. 1b).

2.2. Water sample collection

Samples for phytoplankton pigments were collected from conventional rosettes using Niskin bottles fitted with Teflon-coated closing springs. Primary productivity samples were collected from rosettes which had epoxy-painted frames and were fitted with acid-cleaned Go-Flo bottles (Fitzwater et al., 1982). Samples were collected on stations as ships transited through the iron-fertilized regions. Additionally, discrete fluorometric Chl samples were collected underway from the ships' seawater flow-through systems. Although SF_6 and drifters were deployed to mark the iron-enriched regions (Coale et al., 2004), the gradient of Chl concentrations was used to operationally differentiate In versus Out (or edge) stations (Figs. 2a and b).

2.3. Chl and other pigments

Chl concentrations were determined fluorometrically. Water samples were filtered in parallel onto 25 mm Whatman glass fiber filters (GF/F—nominally a 0.7 μm size fraction), and 5 and 20 μm Poretics polycarbonate filters (25 mm diameter). Volumes filtered were nominally 275 ml for GF/F samples, 1 L for 5 μm samples and 2 L for 20 μm samples in accordance with pigment filtration protocols by Bidigare et al. (2004). Pigments were extracted into 8 ml of 90% acetone for at least 24 h but not more than 48 h in the dark at −20 °C. Fluorescence was measured on a Turner model 10AU fluorometer before and after the addition of 10% HCl. Chl concentrations were calculated from coefficients determined by instrument calibrations performed using a commercially available Chl *a* standard.

Phytoplankton pigment concentrations were determined by high performance liquid chromatography (HPLC) (Bidigare et al., 2004). The suite of pigments analyzed included Chls, photosynthetic carotenoids (PSCs) and photoprotective carotenoids. Chls included Chl *a*, chlorophyllide *a*, Chl *b* and Chl *c*. PSC included peridinin (PER), 19′-butanoyloxyfucoxanthin (BUT), fucoxanthin (FUCO), 19'-hexanoyloxyfucoxanthin (HEX) and prasinoxanthin. Photoprotective carotenoids included violaxanthin, diadinoxanthin, alloxanthin, diatoxanthin, zeaxanthin, α-carotene, and *β*-carotene. Water samples were filtered onto 25 mm diameter Whatman GF/F filters then stored in liquid nitrogen until analyzed. Volumes filtered were 0.5 L for GF/F samples, 2 L for 5 μm samples and 4 L for 20 μm samples (Bidigare et al., 2004).

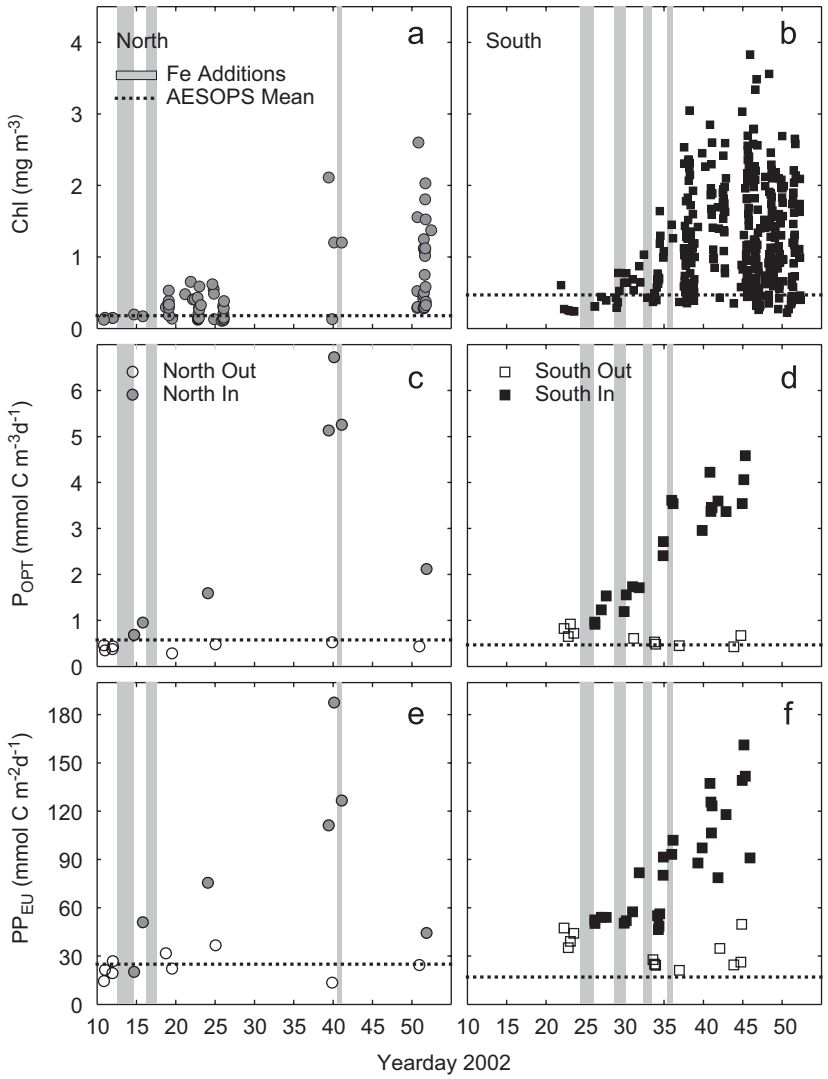

Fig. 2. Time-series of chlorophyll (fluorometric) concentrations and primary productivity in the two iron-enriched patches at 56°S and 66°S. Left panels are Subantarctic Zone (north patch) properties; right panels show properties for the region poleward of the SBACC (south patch). (a, b) Surface chlorophyll *a* from discrete analyses of filtered samples collected from both the CTD stations as well as from the ships' underway seawater systems. IN vs. OUT distinctions have not been made because discrete underway samples were collected during transects through the patches and therefore represent a continuum of OUT, edge and IN values. (c, d) P_{OPT} (mmol C m^{-3} d^{-1}) is the highest water column primary productivity in a 24-h, on-deck, simulated light-level incubation. (e, f) PP_{EU} (mmol C m^{-2} d^{-1}) is the areal primary productivity integrated to the depth at which PAR is 1% of the surface incident irradiance [$E_d(0^-)$]. Gray bars represent the time periods of iron fertilization. The horizontal dotted lines represent the JGOFS AESOPS 1998 late summer mean values of each parameter within each corresponding region (Hiscock et al., 2003).

2.4. Primary productivity

Net primary productivity (PP) was measured using radiolabeled carbon incorporation during 24-h on-deck incubations (Barber et al., 1996). Water samples were collected opportunistically, at any time of day, into sterile 75 ml polystyrene tissue culture flasks and inoculated with ~10 μCi of ^{14}C-carbonate stock solution. For each station, one replicate surface sample for each size fraction was filtered immediately to provide time-zero method controls. Remaining samples were incubated for 24 h on deck in acrylic incubators screened with blue plastic plus neutral density screening to achieve a given percentage of surface irradiance [$E_d(0^-)$], nominally 100%, 50%, 10% and 1% or 100%,

47%, 30%, 16%, 10% and 1%, depending upon incubator availability. The 24-h incubation period integrated diel effects of light availability and cell growth cycles. No dark bottle controls were measured. Incubator temperatures were maintained by a continuous flow of surface seawater. After incubation, parallel samples were filtered onto 25 mm Whatman GF/F filters and 5 and 20 μm Poretics polycarbonate filters then acidified with 0.5 ml of 0.5 N HCl for 24 h to liberate unincorporated inorganic ^{14}C. Ecolume scintillation fluid (7 ml) was added. To determine total added activity, subsamples (0.1 ml) were removed from select inoculated samples prior to filtering and added to a vial containing 0.1 ml β-phenylethylamine and 7 ml of Ecolume scintillation fluid.

P_{OPT} (mmol C m^{-3} d^{-1}) is the maximum productivity per unit volume measured within the water column. Areal productivity (PP_{EU}, mmol C m^{-2} d^{-1}) is the water column productivity integrated through the euphotic zone, defined as the depth to which 1% of the incident photosynthetically active radiation (PAR) just below the surface [$E_d(0^-)$] penetrates. Integrals were determined by summing the trapezoidal areas as defined by the average PP over the change in depth. Photosynthetic performance (P^B_{OPT}, mmol C mg Chl^{-1} d^{-1}) is the highest Chl-normalized productivity in the water column in a 24-h primary productivity incubation. For example, in a water column with uniform Chl distribution P^B_{OPT} will be at the depth with the highest productivity (P_{OPT}) (usually near or just below the surface). Hourly P^B_{OPT} (mmol C mg Chl^{-1} h^{-1}) is daily P^B_{OPT} divided by the photoperiod. Photoperiod is the number of hours from sunrise to sunset minus 2 h to account for acute sun angles to water surface at sunrise and sunset.

The 1% euphotic depth ($z_{EU1\%}$) was determined at the time of the cast using the average attenuation coefficient (K_d) calculated from irradiance measurements made with scalar 4π PAR sensors at several depths throughout the water column for each hydrocast. Widely fluctuating PAR values due to wave focusing effects from near surface depths were excluded (Kirk, 1994). Ships were positioned to minimize ship shadows during hydrocasts (Kirk, 1994). Because skies were overcast during most of the experiment, intermittent cloud effects on PAR measurements (Kirk, 1994) during the shallow biological casts were negligible. Euphotic depths (z_{EU}) during night casts were estimated based on previous daytime values from a similar patch location.

2.5. Size-fraction calculations

As described above, Chl and primary productivity were determined for total phytoplankton as well as for three size classes of phytoplankton. Samples collected on GF/F filters were considered total phytoplankton and samples filtered with 20 μm Poretics filters were considered microplankton (>20 μm) following conventional usage. Although our size-fraction definitions for pico- and nanoplankton differ slightly from conventional usage (<2 μm, and 2 to 20 μm, respectively) we adopt the terms here for brevity. Picoplankton (<5 μm) were determined by subtracting the 5 μm filter values from GF/F values, and nanoplankton (5–20 μm) were determined by subtracting 20 μm filter values from 5 μm filter values.

2.6. Total particulate organic carbon (POC) to Chl ratio

Total POC data from the SOFeX data website (http://www.mbari.org/sofex/) were used with the permission of Craig Hunter (Moss Landing Marine Laboratories), Mark Altabet and David Timothy (University of Massachusetts—Dartmouth) to calculate POC:Chl ratios. POC was measured following JGOFS protocols (Kadar et al., 1993; Altabet and Francois, 2001). Because the POC samples were not necessarily collected from the same hydrocast bottles as the Chl samples, the mean POC values of the upper 50 m were divided by the upper 50 m mean Chl values to calculate POC:Chl (g:g) for each station where both measurements were available.

3. Results

3.1. Physico-chemical conditions and iron enrichment

A brief overview of the physico-chemical conditions is provided here. Further details can be found in Coale et al. (2004). The Subantarctic Zone surface temperatures ranged from 6.5 to 9 °C, nitrate was ~21 mmol m^{-3} while silicic acid concentration in the surface was ~2.0 mmol m^{-3} (data from http://www.mbari.org/sofex/). North patch iron enrichment achieved about 1.2 μmol m^{-3} dissolvable iron or about 10x ambient concentration

(0.09–0.13 μmol m^{-3}) in the surface. In contrast, the south patch, poleward of the SBACC, was much colder with higher concentrations of both nitrate and silicic acid. Surface temperatures ranged from −0.2 to −0.7 °C. Mean surface concentrations of nitrate and silicic acid were ~27 and ~64 mmol m^{-3}, respectively (data from http://www.mbari.org/sofex/). Surface iron concentration inside the patch reached twice that of ambient iron or about 0.7 compared to 0.2–0.4 μmol m^{-3} (Coale et al., 2004). At both sites, macronutrient drawdown by phytoplankton was evident but tempered by entrainment of nearby ambient waters (Coale et al., 2004; Hiscock and Millero, 2005). Mixed layer depths were well defined and relatively shallow (with respect to Sverdrup's critical depth criterion) at about 40 m in the Subantarctic Zone and about 45 m poleward of the SBACC. Notably, mixed-layer depths were unaffected by short term variations in wind speed, which ranged from 12 to 30 m s^{-1} in the north patch and from 7 to 35 m s^{-1} in the south patch (Coale et al., 2004).

3.2. Subantarctic Zone (north patch)

3.2.1. Total Chl (fluorometric) and primary productivity (Subantarctic Zone—north patch)

Total Chl concentrations and primary productivity increased dramatically in response to iron enrichment. Maximum Chl concentrations and primary productivity were observed 25–26 d after initial fertilization. Total Chl in the iron-enriched surface layer increased 12-fold at stations in the experimental patch relative to ambient Chl concentrations outside the patch. Surface Chl increased from 0.17 mg m^{-3} prior to iron addition to 2.1 mg m^{-3} (Table 1) while ambient concentrations outside the patch were unchanged. Underway, discrete Chl measurements ranged even higher, to 2.6 mg m^{-3} (Fig. 2a). Primary productivity responded to repeated iron additions with about a 15-fold increase in the maximal water column productivity (P_{OPT}) and an 8-fold increase in the integrated water column productivity (PP_{EU}). P_{OPT} increased from a mean of 0.44 mmol C m^{-3} d^{-1} outside the patch to a maximum of 6.7 mmol C m^{-3} d^{-1} observed within the patch. The depths of most P_{OPT} observations were near the surface both in and out of the iron-enriched patch (Fig. 4a). PP_{EU} increased from a mean OUT value of about 23 mmol C m^{-2} d^{-1} to a maximum of 188 mmol C m^{-2} d^{-1} (Table 1; Figs. 2c and e).

3.2.2. Size-fractionated Chl (fluorometric) and primary productivity (Subantarctic Zone—north patch)

Surface Chl, P_{OPT} and PP_{EU} increased in the iron-enriched north patch for all three size fractions measured (Table 1; Figs. 3 and 4). Picoplankton, the smallest size fraction, had modest increases in Chl and primary productivity. Chl reached a maximum of 0.36 mg m^{-3} compared to the mean OUT value of 0.12 mg m^{-3}, while P_{OPT} reached over 2 mmol C m^{-3} d^{-1} compared to the mean OUT value of 0.32 mmol C m^{-3} d^{-1}. The mid-sized nanoplankton Chl increased to 0.29 mg m^{-3} from 0.04 mg m^{-3}. Nanoplankton P_{OPT} increased to 2.8 mmol C m^{-3} d^{-1} from about 0.1 mmol C m^{-3} d^{-1}. Chl in the largest microplankton size fraction increased about 100-fold to more than 1 mg m^{-3} compared to the mean OUT value of 0.011 mg m^{-3}. Microplankton P_{OPT} reached about 2 mmol C m^{-3} d^{-1} compared to the mean OUT value of 0.044 mmol C m^{-3} d^{-1}.

3.2.3. Composition of phytoplankton size-fraction assemblage (Subantarctic Zone—north patch)

The composition of the phytoplankton size assemblage changed significantly in response to iron enrichment in the north patch. The proportional size-fraction distribution of phytoplankton Chl in ambient waters prior to iron addition and outside of the iron-enriched patch was 70% picoplankton, 24% nanoplankton and 6% microplankton Chl (Table 1 and Figs. 5a and 6a). The ambient proportion of both total P_{OPT} and total PP_{EU} was about 72% picoplankton, 19% nanoplankton and about 9% microplankton productivity (Table 1 and Figs. 6c and e). In response to iron enrichment the new proportional composition of total Chl was 15% picoplankton, 19% nanoplankton and 66% microplankton Chl (Table 1 and Figs. 5a and 6a). The new, iron-enriched proportional composition of total P_{OPT} and total PP_{EU} was about 36% picoplankton, 33% nanoplankton and about 31% microplankton productivity (Table 1 and Figs. 6c and e). In summary, the dominant size fraction for Chl changed from picoplankton to microplankton with iron enrichment in the north patch. Picoplankton dominated primary productivity under ambient conditions and iron addition resulted in a new distribution of primary productivity that was about equal among the three size fractions.

Table 1
North patch surface chlorophyll (fluorometric) and primary productivity determined at OUT and IN stations of the iron enrichment experiment established in the Subantarctic Zone at 56°S

Subantarctic zone (north patch)				
	Size fraction Property			
	Total	<5 μm	5–20 μm	>20 μm
	Surface chlorophyll ($mg\,m^{-3}$)			
Out				
Mean of all OUT ± SE	0.17 ± 0.02	0.12 ± 0.01	0.040 ± 0.01	0.011 ± 0.003
% of normalized total		70	24	6
Min–max	0.12–0.29	0.090–0.19	0.010–0.12	0.0058–0.030
n	9	9	9	9
In				
Mean of three max full IN PP stations ± SE	1.5 ± 0.3	0.23 ± 0.05	0.28 ± 0.002	0.98 ± 0.2
% of normalized total		15	19	66
Min—max range of all IN PP stations	0.17–2.1	0.13–0.36	0.029–0.29	0.0081–1.5
n of all	7	7	7	6
	P_{opt} ($mmol\,C\,m^{-3}\,d^{-1}$)			
Out				
Mean of all OUT ± SE	0.44 ± 0.04	0.32 ± 0.04	0.095 ± 0.01	0.044 ± 0.007
% of normalized total		70	21	9
Min—max	0.28–0.68	0.16–0.49	0.043–0.18	0.014–0.085
n	9	9	9	9
In				
Mean of three max full IN PP stations ± SE	5.7 ± 0.3	2.2 ± 0.3	2.1 ± 0.4	1.9 ± 0.1
% of normalized total		35	34	31
Min—max range of all IN PP stations	0.33–6.7	0.22–2.8	0.11–2.8	0.042–2.1
n of all	7	7	7	7
	PP_{EU} ($mmol\,C\,m^{-2}\,d^{-1}$)			
Out				
Mean of all OUT ± SE	23 ± 3	17 ± 2	3.9 ± 0.7	2.2 ± 0.3
% of normalized total		74	17	9
Min—max	13–37	10–32	1.4–8.1	1.0–4.3
n	9	9	9	9
In				
Mean of three max full IN PP stations ± SE	142 ± 23	51 ± 8.5	44 ± 13	47 ± 1.8
% of normalized total		36	31	33
Min–max range of all IN PP stations	20–188	13–67	5.2–70	2.3–50
n of all	7	7	7	7

Chlorophyll values are from the surface bottles at productivity stations only and do not include discrete underway observations. OUT values are from all OUT productivity stations. IN values are represented in two ways: (1) the mean and standard error are calculated from three maximum productivity IN stations where all size fractions were measured ("full" stations) and (2) the range (min–max) of given parameters are from all IN productivity stations. Abbreviations: n is number of observations; SE is standard error.

3.3. Poleward of the SBACC (south patch)

3.3.1. Total Chl (fluorometric) and primary productivity (poleward of SBACC—south patch)

Total Chl and primary production increased in response to iron enrichment in the high silicic acid south patch poleward of the SBACC. Maximum Chl concentrations and primary productivity were observed at the final stations 20–21 d after initial iron fertilization. Surface layer Chl increased 10-fold, ranging from $0.4\,mg\,m^{-3}$ prior to iron addition and outside of the iron-enriched patch to

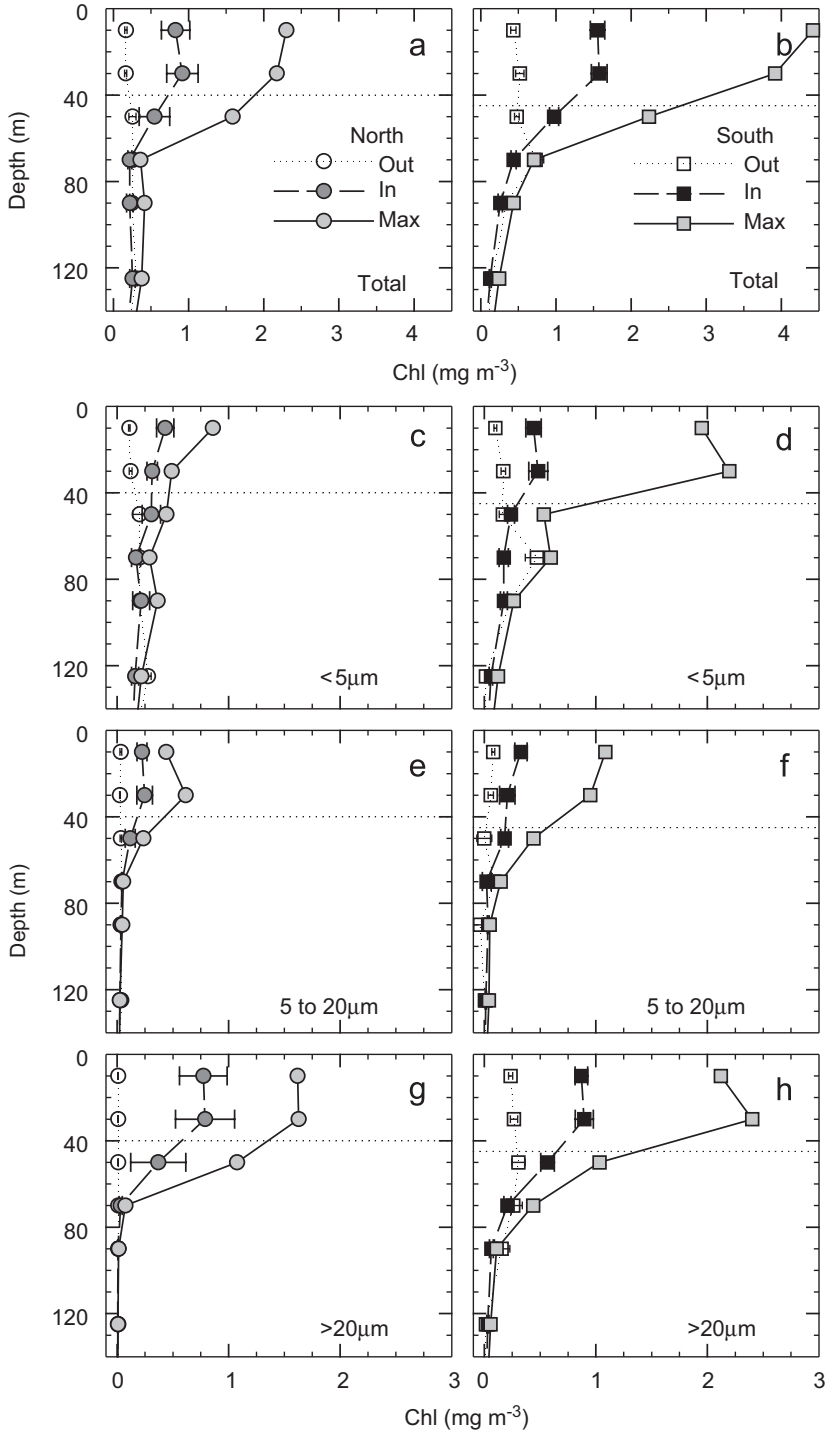

Fig. 3. Depth profiles of mean chlorophyll (fluorometric; mg m^{-3}) for mean OUT and mean of three IN stations (as defined for Tables 1 and 2) along with maximum observed IN values binned by 20 m depth intervals. North patch is on the left panels, south patch is on the right panels (a, b = total; c, d = <5 µm; e, f = 5–20 µm; g, h = >20 µm). Samples were filtered onto GF/F filters and 5 and 20 µm polycarbonate filters. Size fractions were calculated by subtraction (see Section 2). Note that the chlorophyll scale changes between the total and size-fraction plots. Error bars are standard error of the mean. Dotted horizontal lines are approximate mixed layer depths.

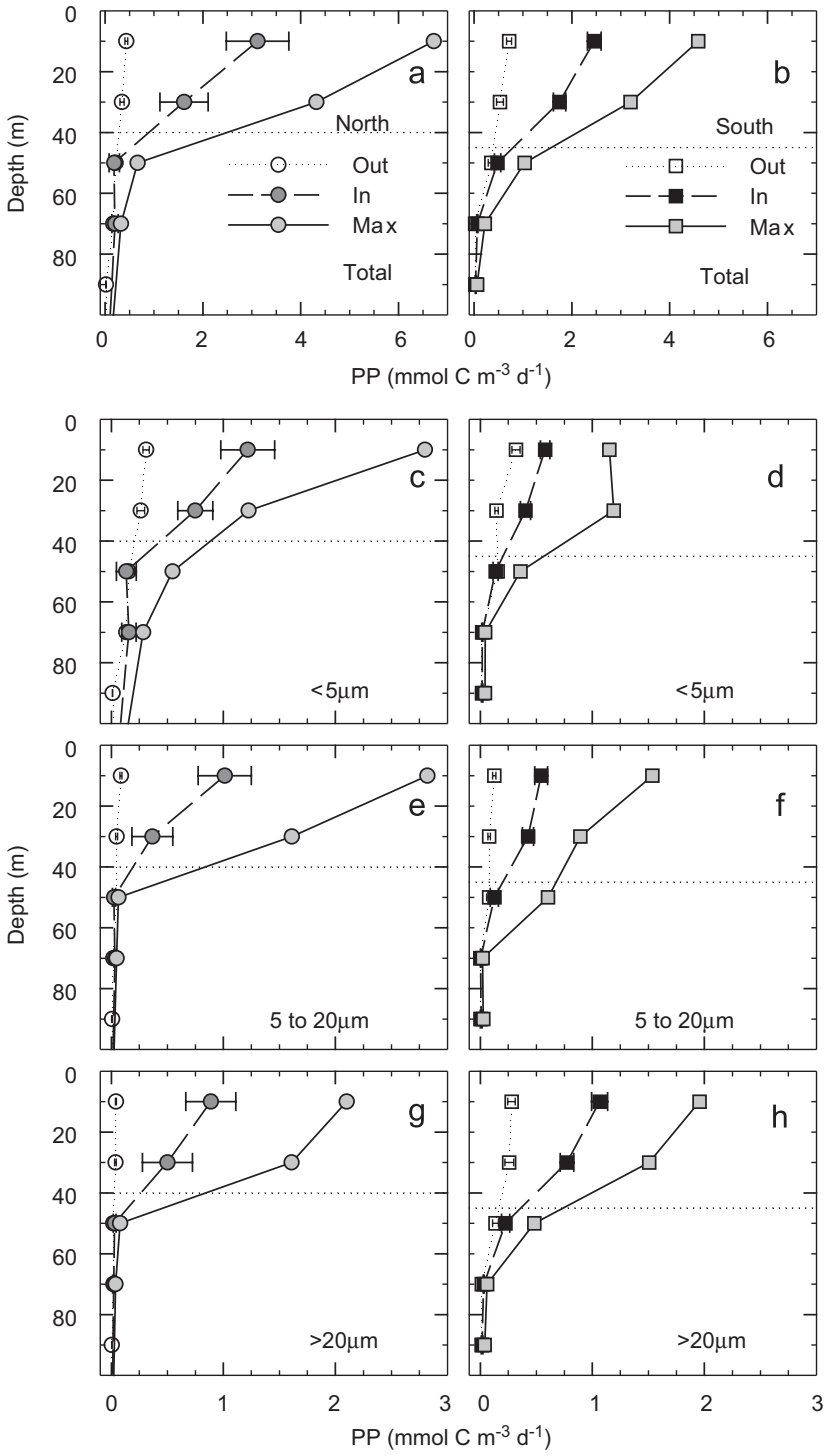

Fig. 4. Depth profiles of mean primary productivity (PP) (mmol C m^{-3} d^{-1}) for mean OUT and mean of three IN stations (as defined for Tables 1 and 2) along with the maximum observed IN values binned by 20 m depth intervals. North patch is on the left panels, south patch is on the right panels. (a, b) Total particulate primary productivity is that retained on a GF/F filter. Size fractions of PP are shown as follows: (c, d) <5 µm; (e, f) 5–20 µm; (g, h) >20 µm. Note PP scale change between the total and size-fraction plots. Error bars are standard error of the mean. Dotted horizontal lines are approximate mixed layer depths.

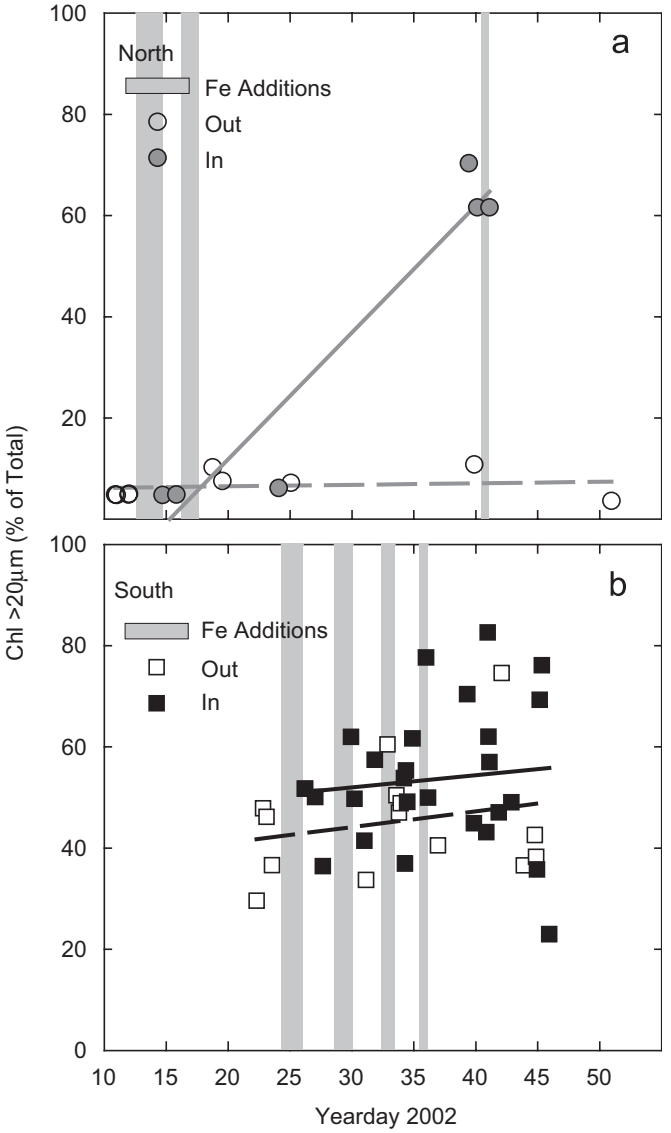

Fig. 5. Time series of the percentage of total chlorophyll (fluorometric) represented in the >20 µm size fraction for (a) the north patch and (b) the south patch. Solid lines are linear regressions for IN values; dashed lines are linear regressions for OUT values. Neither the IN nor the OUT south patch regression slope is statistically different from zero.

3.8 mg m^{-3} (Table 2; Fig. 2b). Primary productivity responded to iron enrichment with about a 5-fold increase. P_{OPT} increased from a mean of 0.73 mmol C m^{-3} d^{-1} outside the patch to a maximum of 4.6 mmol C m^{-3} d^{-1} within the patch (Table 2; Fig. 2d). The depths of most P_{OPT} were observed to be near the surface both in and out of the iron-enriched patch (Fig. 4b). Mean PP_{EU} outside the patch was about 33 mmol C m^{-2} d^{-1} and increased to a maximum of 161 mmol C m^{-2} d^{-1} 23 d after iron addition (Table 2; Fig. 2f). As for the north patch, south patch enrichment effects within the water column were confined to the mixed-layer depth, which was approximately 45 m in the south patch (Fig. 3).

3.3.2. Size-fractionated Chl (fluorometric) and primary productivity (poleward of SBACC—south patch)

Surface Chl, P_{OPT} and PP_{EU} increased in the iron-enriched south patch for all three size fractions measured (Table 2; Figs. 3 and 4). Picoplankton Chl

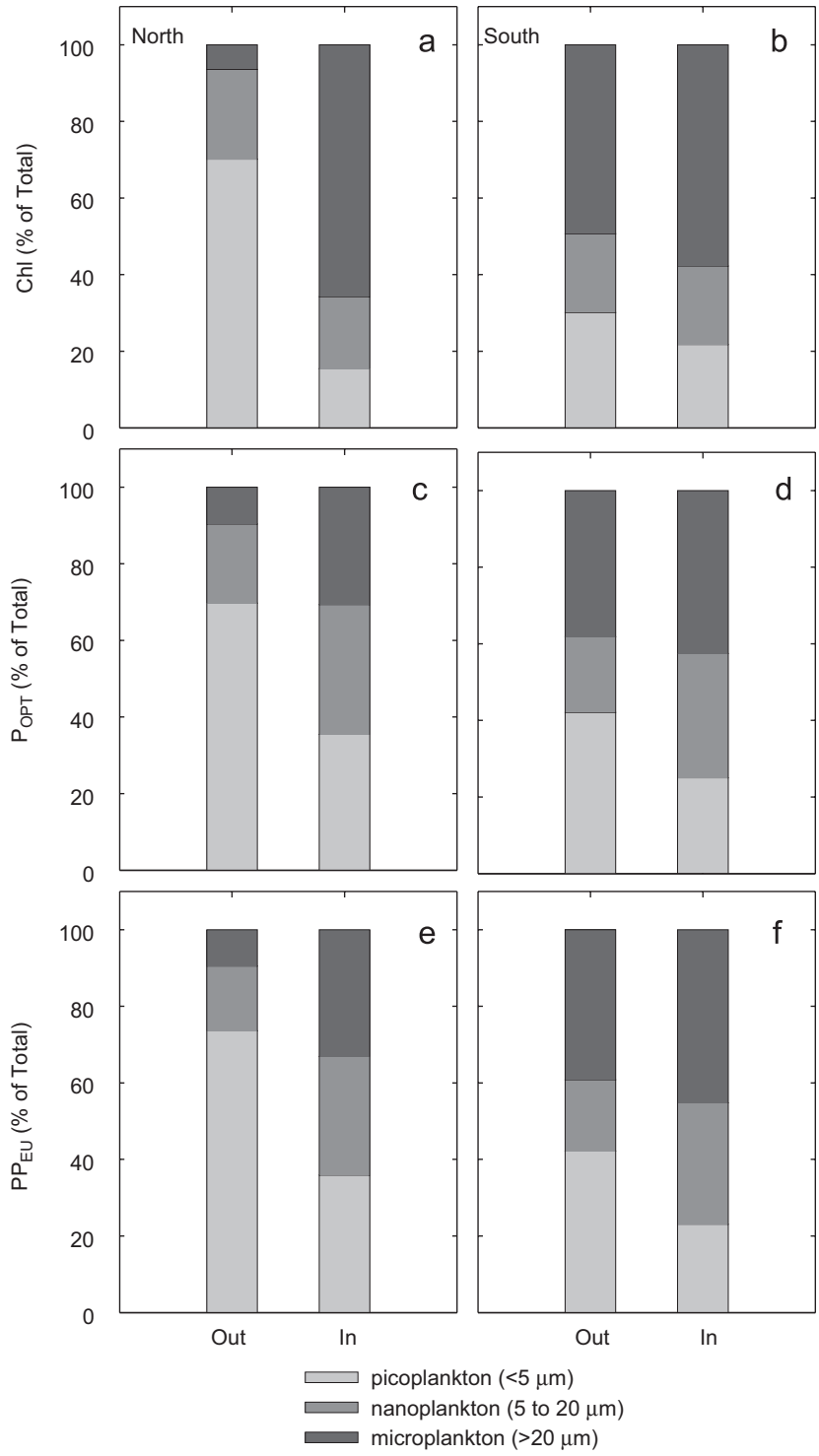

Fig. 6. Proportional representation of (a, b) chlorophyll, (c, d) P_{OPT} and (e, f) PP_{EU} of each of the three size classes measured. Left panels are north patch; right panels, south patch. OUT bars are means of all out stations for a given patch and parameter. IN bars are the means of three maximum productivity stations where all parameters for all size fractions were measured.

Table 2
South patch surface chlorophyll (fluorometric) and primary productivity determined at OUT and IN stations of the iron enrichment experiment established in the region poleward of the SBACC at 66°S

Poleward of the SBACC (south patch)				
	Size fraction Property			
	Total	<5 μm	5–20 μm	>20 μm
	Surface chlorophyll (mg m^{-3})			
Out				
Mean of all OUT±SE	0.41±0.05	0.11±0.008	0.075±0.01	0.18±0.02
% of normalized total		30	20	50
Min—max	0.24–0.89	0.085–0.16	0.031–0.14	0.0058–0.030
n	12	9	9	12
In				
Mean of three max full IN PP stations±SE	1.6±0.3	0.35±0.05	0.33±0.2	0.93±0.2
% of normalized total		22	20	58
Min—max range of all IN PP stations	0.31–3.8	0.041–1.9	0.00–1.1	0.14–1.6
n of all	28	20	20	27
	P_{opt} (mmol C m^{-3} d^{-1})			
Out				
Mean of all OUT±SE	0.73±0.08	0.32±0.05	0.15±0.03	0.29±0.05
% of normalized total		42	20	38
Min–max	0.43–1.4	0.12–0.53	0.036–0.28	0.079–0.72
n	12	9	9	12
In				
Mean of three max full IN PP stations±SE	3.5±0.07	1.0±0.2	1.3±0.2	1.7±0.07
% of normalized total		25	33	43
Min–max range of all IN PP stations	0.92–4.6	0.18–1.2	Bd—1.5	0.23–2.0
n of all	28	19	19	27
	PP_{EU} (mmol C m^{-2} d^{-1})			
Out				
Mean of all OUT±SE	33±3	14±3	6.2±1	13±2
% of normalized total		42	19	39
Min–max	21–50	6.4–25	2.3–13	5.1–26
n	12	9	9	12
In				
Mean of three max full IN PP stations±SE	104±7	24±0.6	33±6	47±4
% of normalized total		23	32	45
Min–max range of all IN PP stations	47–161	7.7–36	Bd–29	9.5–65
n of all	28	19	19	27

Chlorophyll values are from the surface bottles at productivity stations only and do not include discrete underway observations. OUT values are from all OUT productivity stations. IN values are represented in two ways: (1) the mean and standard error are calculated from three maximum productivity IN stations where all size fractions were measured (''full'' stations) and (2) the range (min–max) of given parameters are from all IN productivity stations. Abbreviations: *n* is number of observations; SE is standard error; Bd is below detection.

reached a maximum of 1.9 mg m^{-3} compared to the mean OUT value of 0.11 mg m^{-3}, and picoplankton P_{OPT} reached 1.2 mmol C m^{-3} d^{-1} compared to the mean OUT value of 0.32 mmol C m^{-3} d^{-1}. Nanoplankton Chl increased to a maximum of 1.1 mg m^{-3} from the mean OUT of 0.075 mg m^{-3}, and nanoplankton P_{OPT} increased to 1.5 mmol C m^{-3} d^{-1} from 0.15 mmol C m^{-3} d^{-1} mean OUT. Microplankton Chl increased 9-fold to 1.6 mg m^{-3} compared to the mean OUT value of 0.18 mg m^{-3}, while microplankton

P_{OPT} reached about 2 mmol C m^{-3} d^{-1} compared to the mean OUT value of 0.29 mmol C m^{-3} d^{-1}.

3.3.3. Composition of phytoplankton size-fraction assemblage (poleward of SBACC—south patch)

Whereas iron enrichment in the north patch resulted in a significant shift of the phytoplankton size assemblage from picoplankton-dominant to microplankton-dominant, iron enrichment did not markedly alter the proportional makeup of the phytoplankton size-fraction assemblage over the duration of study in the south patch. The proportional size-fraction distribution of total phytoplankton Chl in ambient waters prior to iron addition and outside of the iron-enriched patch was 30% picoplankton Chl, 20% nanoplankton Chl and 50% microplankton Chl (Table 2 and Figs. 5b and 6b). The ambient proportion of both total P_{OPT} and total PP_{EU} was about 42% picoplankton productivity, 20% nanoplankton productivity and about 38% microplankton productivity (Table 2 and Figs. 6d and f). In response to iron enrichment, the new proportional composition of total Chl was 22% picoplankton Chl, 21% nanoplankton Chl and 57% microplankton Chl (Table 2 and Figs. 6d and f). The new, iron-enriched proportional composition of total P_{OPT} and total PP_{EU} was about 24% picoplankton productivity, 32% nanoplankton productivity and about 44% microplankton productivity (Table 1 and Figs. 6c and e). Overall, while the concentrations of Chl and the rates of primary production increased with iron addition, the proportional distribution of Chl and primary productivity throughout the three size classes remained relatively unchanged in the south patch.

3.4. HPLC pigment compositions (north and south patches)

In both the north and the south patches, iron enrichment resulted in increases in the absolute concentrations of four of the five PSC pigments measured: PER, BUT, FUCO and HEX (Figs. 7a and b). Prasinoxanthin was undetectable in the mixed layers and was present in concentrations less than 7 μg m^{-3} below the mixed layer both IN and OUT of the iron-enriched north and south patches. Over time, the concentration of PSCs increased

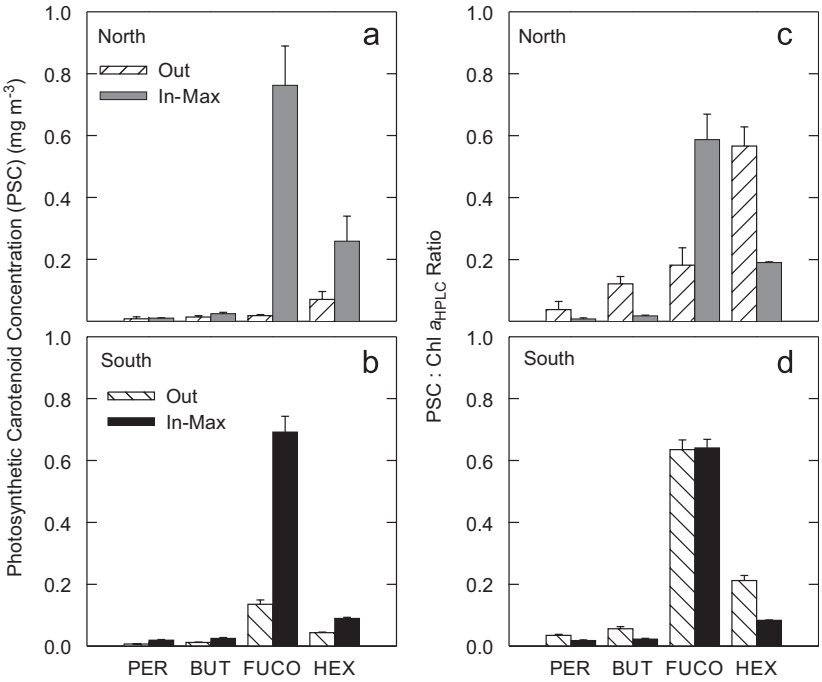

Fig. 7. HPLC-determined carotenoids in absolute concentration (mg m^{-3}) for (a) north patch and (b) south patch and HPLC-determined carotenoid-to-chlorophyll *a* ratios (g:g) for (c) north patch and (d) south patch. OUT values are means for the entire experimental period. IN values are means of 3 maximum productivity stations as described in Tables 1 and 2. Error bars are standard error of the mean. PER, Peridinin; BUT, 19′-Butanoyloxyfucoxanthin; FUCO, Fucoxanthin; HEX, 19′-Hexanoyloxyfucoxanthin.

faster than the concentration of photoprotective carotenoids in both north and south experiments (data not shown).

While absolute PSC concentrations increased in both north and south patches, the changes in Chl-normalized concentrations serve to differentiate the responses of each region to iron addition (Figs. 7c and d). In the Subantarctic north patch, iron enrichment dramatically shifted the dominant PSC from HEX, a pigment marker for prymnesiophytes, to FUCO, the marker for diatoms (Fig. 7c). This shift is quite apparent in the time series of diatom Chl (Letelier et al., 1993) as a percentage of total Chl (Fig. 8a). In contrast, FUCO was the dominant PSC both in and out of the iron-enriched south patch and the Chl-normalized relationships among the PSCs changed very little (Fig. 7d). The percentage of diatom Chl in the south patch was rather variable over time, ranging from about 40% to 60% outside of the iron-enriched south patch and from 40% to 65% within the iron-enriched area (Fig. 8b).

3.5. Non-photosynthetic chloropigments

The ratio of fluorometric Chl to HPLC-determined Chl *a* ranged from 1:1 to 3:1 depending upon patch location, depth, and iron-enriched Chl biomass. The ambient ratio of fluorescent chloropigments to HPLC-determined Chl *a* in the north patch was only slightly elevated in the upper 40–50 m, specifically 1.1:1, compared to the ratio in deeper water, which was 1:1 (Fig. 9a). This minor disparity in the mixed layer was eliminated by adding the concentration of chlorophyllide *a* to the HPLC-determined Chl *a* concentration (Fig. 9c). Iron enrichment had no effect on the extent or distribution of these ratios in the north (Fig. 9a). In contrast to the north patch, the ambient south patch ratios in the upper 40–50 m were initially about 1.7:1. This ratio increased inside the iron-enriched south patch as the experimental patch developed and reached a ratio of 3:1 in the near surface waters late in the experiment when Chl biomass was at its highest observed values (Fig. 9b). A second-order polynomial regression fit the empirical change in ratio as a function of time in the south patch, while second-order equations did not substantially improve upon linear regression models for the north patch. The addition of chlorophyllide *a* to HPLC Chl *a* reduced the discrepancy in the south patch somewhat but was not sufficient to explain the difference entirely (Fig. 9d). Chl *b* was usually undetectable near the surface waters, which is where the non-photosynthetic fluorescent chloropigments showed the most effect.

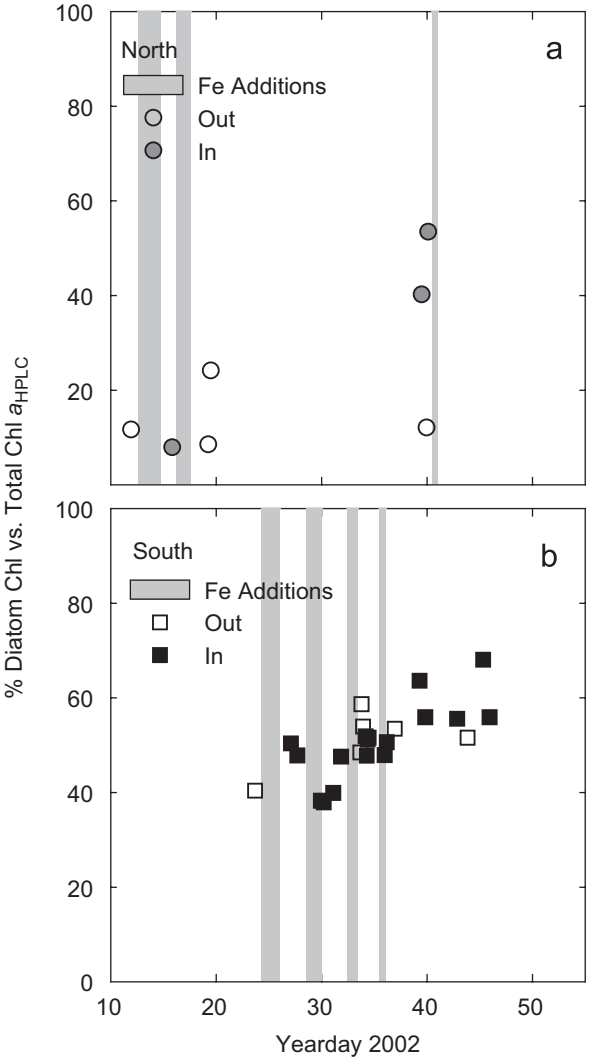

Fig. 8. Time series of diatom chlorophyll (Letelier et al., 1993) as a percentage of total chlorophyll in the (a) north patch and (b) south patch.

3.6. Photosynthetic performance

Because HPLC Chl *a* measurements were not available for every primary productivity station, we estimated the parameter Chl^{*}_{HPLC} by fitting total fluorometric Chl values to the regressions described above. P^{B*}_{OPT} is P_{OPT} normalized to Chl^{*}_{HPLC} and is used to determine photosynthetic performance.

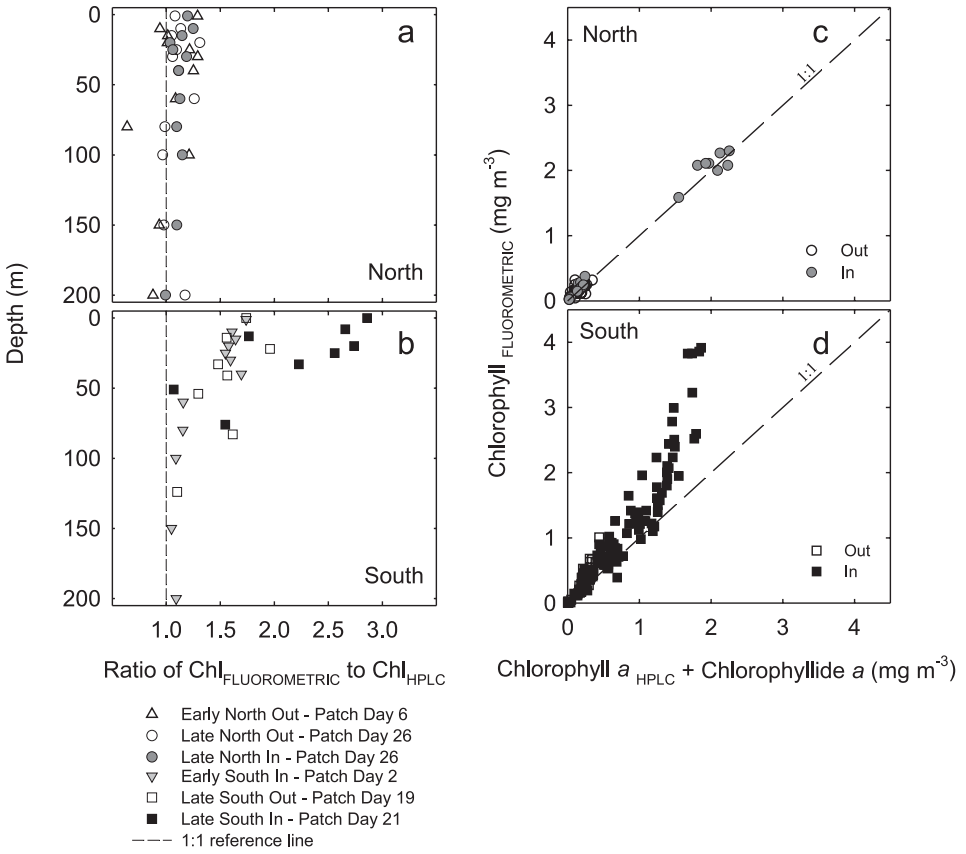

Fig. 9. Representative depth profiles of the ratio of fluorometrically determined chlorophyll to HPLC-determined chlorophyll *a* concentrations in the north patch (a) and south patch (b). Patch days refer to days since first iron fertilization in each patch. Dashed vertical lines represent the ratio of 1:1. (c) North patch and (d) south patch regressions of fluorometrically determined chlorophyll versus the sum of chlorophyll *a* and chlorophyllide *a* as determined by HPLC. Dashed diagonal lines represent the 1:1 ratio. In the north patch (c), the addition of chlorophyllide *a* to the HPLC chlorophyll *a* makes the ratio 1:1. In the south patch (d) chlorophyllide *a* improves the regression but does not make the ratio 1:1.

P^{B*}_{OPT} was highly variable in the north patch. The limited number of observations showed no detectable change as a result of iron addition (Table 3). Total P^{B*}_{OPT} ranged from 2.1 to 4.4 mmol C mg Chl^{*-1}_{HPLC} d^{-1} outside the patch compared to 2.0–6.7 mmol C mg Chl^{*-1}_{HPLC} d^{-1} within the iron-enriched patch.

Unlike the north patch, a distinct response to iron addition was evident in measurements of total daily photosynthetic performance (P^{B*}_{OPT}) made in and outside of the iron-enriched south patch. Although IN and OUT P^{B*}_{OPT} values are variable (Table 3), both values tend to decrease throughout the course of the experiment from about 5–6 mmol C mg Chl^{*-1}_{HPLC} d^{-1} to about 2–3 mmol C mg Chl^{*-1}_{HPLC} d^{-1} with the decrease being less pronounced within the iron-enriched waters (Figs. 10a and b). Daily PAR did not decrease systematically over this same period and so could not explain this decline of P^{B*}_{OPT} (not shown). To account for the effect of rapidly diminishing photoperiod as the south patch experiment progressed during the early fall season at this high latitude (66°S), daily P^{B*}_{OPT} was converted to hourly P^{B*}_{OPT} (mmol C mg Chl^{*-1}_{HPLC} h^{-1}), then plotted against photoperiod. As photoperiod decreased, hourly P^{B*}_{OPT} significantly decreased in the ambient phytoplankton ($p = 0.004$; Fig. 9c) but was not correlated within the iron-enriched assemblage (Fig. 10d). In the ambient waters outside the south patch hourly P^{B*}_{OPT} was not a function of daily PAR (Fig. 10e); however, within the iron-enriched patch hourly P^{B*}_{OPT} tended to increase with higher daily PAR albeit with a relatively poor r^2 relationship (>0.3; Fig. 10f).

Table 3
Daily and hourly photosynthetic performance determined using HPLC-corrected fluorometric chlorophyll values ($Chl_{HPLC}*$) for both north and south patches

	Daily P^{B*}_{OPT} (mmol C mg Chl^{*-1}_{HPLC} d^{-1})	Hourly P^{B*}_{OPT} (mmol C mg Chl^{*-1}_{HPLC} h^{-1})
Subantarctic Zone (*north patch*)		
Out		
Mean of all OUT ± SE	3.2 ± 0.3	0.22 ± 0.02
Min—max	2.1–4.4	0.16–0.33
n	9	9
In		
Mean of three max full IN PP stations ± SE	4.9 ± 1	0.37 ± 0.09
Min—max range of all IN PP stations	2.0–6.7	0.15–0.51
n of all	7	7
Poleward of the SBACC (*south patch*)		
Out		
Mean of all OUT ± SE	3.1 ± 0.4	0.19 ± 0.02
Min—max	1.6–5.9	0.098–0.34
n	12	12
In		
Mean of three max full IN PP stations ± SE	3.9 ± 0.5	0.25 ± 0.03
Min—max range of all IN PP stations	1.7–6.2	0.11–0.37
n of all	28	28

Hourly P^{B*}_{OPT} is daily P^{B*}_{OPT} normalized to photoperiod. OUT values are from all OUT productivity stations. IN values are represented in two ways: 1) the mean and standard error are calculated from three maximum productivity IN stations where all size fractions were measured (''full'' stations) and 2) the ranges (min–max) of given parameters are from all IN productivity stations. The north patch stations used in this table are the same as those used in Table 1. The south patch stations used in this table are the same as those used in Table 2. Abbreviations: *n* is number of observations; SE is standard error.

3.7. POC to Chl ratios

In the iron-enriched south patch POC increased at a faster rate than Chl^{*}_{HPLC} (Fig. 11a). The mean of ambient POC:Chl^{*}_{HPLC} was 278 (±13 standard error, $n = 6$). Iron addition considerably reduced the ratio of POC:Chl^{*}_{HPLC} in the south patch to about 100 over the course of the 27 d of observations (Fig. 11b). The limited number of north patch observations was insufficient to characterize the POC:Chl^{*}_{HPLC} response to iron in the Subantarctic region.

4. Discussion and conclusions

4.1. Total and size-fractionated Chl (fluorometric) and primary productivity (north and south patches)

Total Chl concentrations and primary productivity found initially and in subsequent OUT stations of the SOFeX Subantarctic north patch were similar to those observations made in the Subantarctic Zone during the 1997–1998 US Joint Global Ocean Flux Study—Antarctic Ecosystem Southern Ocean Process Studies program (AESOPS) (Hiscock et al., 2003) (Fig. 2) and increased dramatically in response to iron enrichment. As with the north patch, SOFeX south patch Chl concentrations and primary productivity found initially and in subsequent OUT stations were similar to comparable observations made in the region poleward of the SBACC during AESOPS (Hiscock et al., 2003). However, while the Subantarctic north patch phytoplankton response to iron addition exceeded expectations given the potentially limiting silicic acid concentrations, the increases in Chl and primary productivity in response to iron enrichment in the south patch poleward of the SBACC, although impressive, were less than might be expected given the high concentrations of silicic acid availability.

The depth to which iron-enrichment effects were observed within the water column generally matched the average mixed-layer depths in both the north and south patches (Figs. 3 and 4). The profile and PP_{EU} results reported here differ slightly from those we reported in Coale et al. (2004) where PP_{EU} was determined by using a Chl-dependent

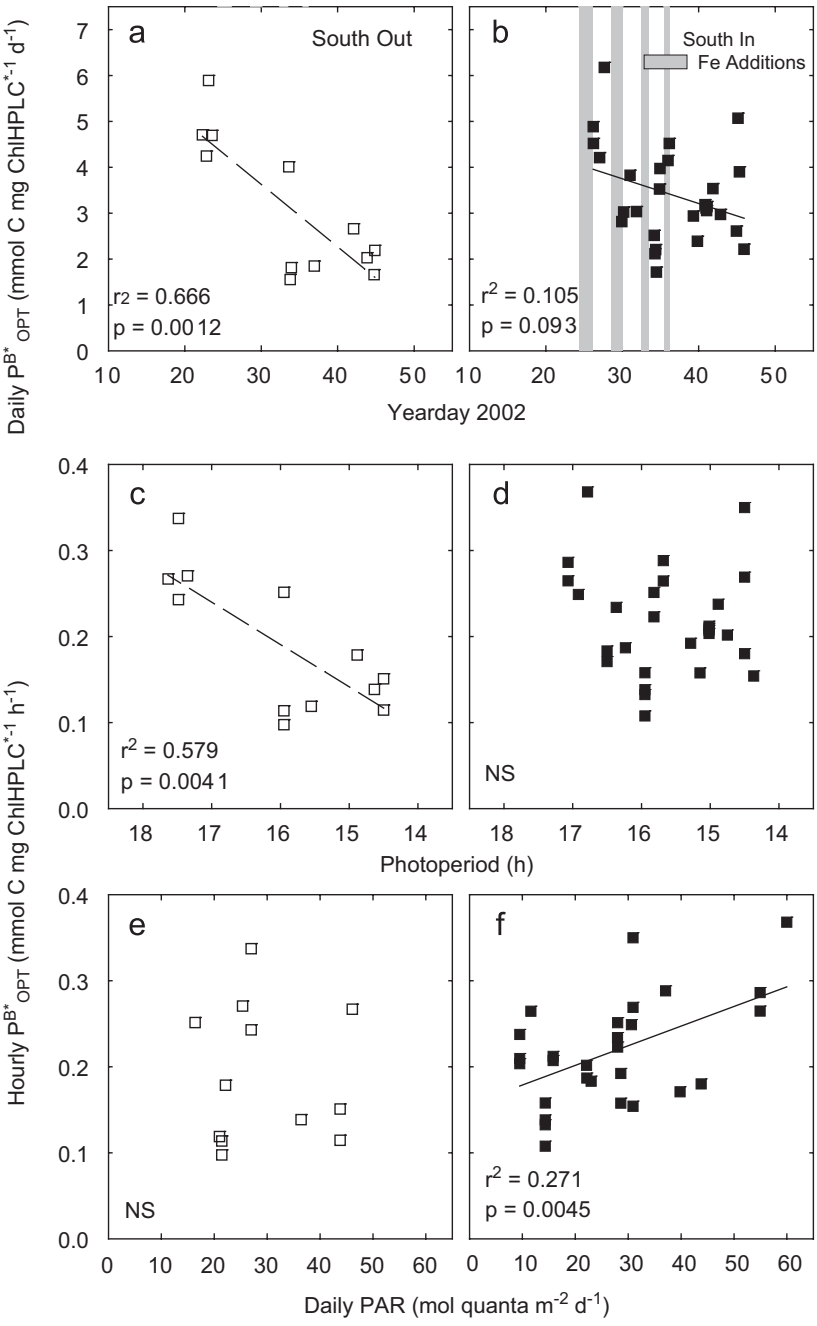

Fig. 10. Daily P^{B*}_{OPT} time series for (a) ambient outside and (b) inside iron-enriched south patch. Hourly P^{B*}_{OPT} with respect to photoperiod (c, OUT and d, IN) and with respect to daily PAR (e, OUT and f, IN). Lines are linear regressions. NS indicates regression slope is not significantly different from zero.

optical model (Morel, 1988) to derive $z_{EU1\%}$. Morel's (1988) model has served very well for determining z_{EU} in tropical and subtropical oligotrophic waters (Barber et al., 1997; Morel and Maritorena, 2001); however, a discrepancy between the Morel-modeled z_{EU} and the K_d-estimated z_{EU} in the SOFeX data suggested a reconsideration of methods. The Morel-modeled depths were overall about 60–80% of the K_d-estimated sample depths depending on patch conditions. For a limited

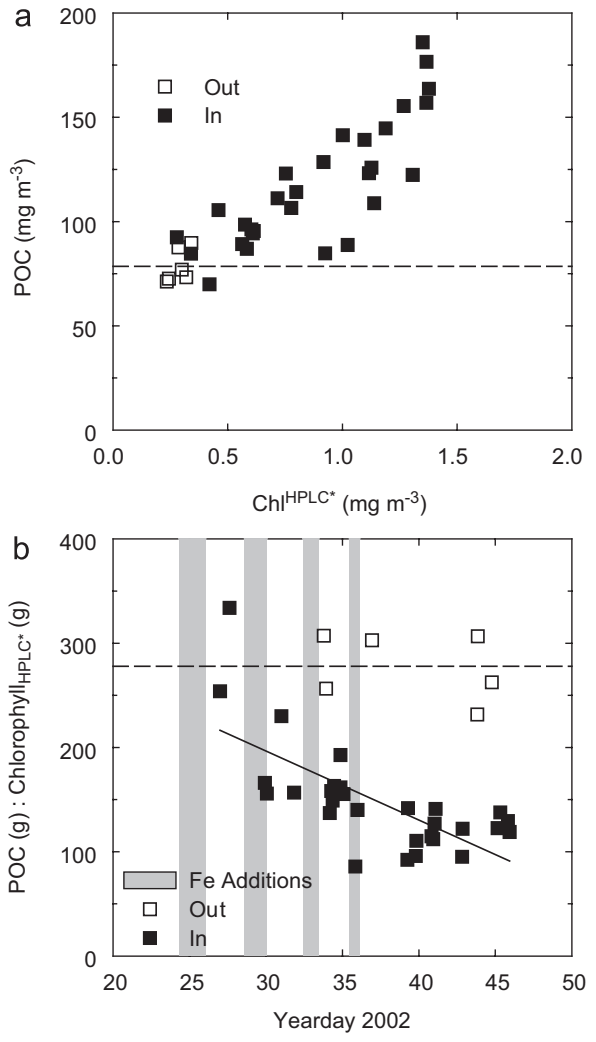

Fig. 11. (a) POC as a function of Chl^{*}_{HPLC} and (b) time series of POC:Chl^{*}_{HPLC} (g:g) ratios in the south patch poleward of the SBACC. Dashed line is the mean OUT value. Solid line is a linear regression of IN values.

number of near noon stations, we had appropriate data with which to determine the actual depth at which PAR measured with the submerged spherical 4π collector was 1% of measured shipboard cosine irradiance. The Morel-modeled depths were about 78% of the measured $z_{EU1\%}$. Bracher and Tilzer (2001) suggested alternative spectral absorption models for particular regions of the Atlantic sector of the Southern Ocean; however, none of the nutrient conditions or phytoplankton assemblages represented in their models appropriately described the SOFeX nutrient and biotic conditions. Revised models for standardizing the method for determining z_{EU} in the diverse regions of the Southern Ocean are needed in order to make comparisons of PP_{EU} and to resolve the extent to which "self-shading" of primary production (Coale et al., 2004) occurs in the water column.

4.2. Significance of the results of size fraction and phytoplankton pigment compositions (north and south patches)

4.2.1. Significant change to the proportional composition of size fractions and phytoplankton pigments in the Subantarctic Zone north patch

The composition shift toward larger phytoplankton and diatom dominance which was seen in the north patch experiment has been common among most in situ HNLC iron-enrichment experiments (Coale et al., 1996; Boyd et al., 2000; Gervais et al., 2002; Tsuda et al., 2003; Boyd et al., 2004; de Baar et al., 2005). Importantly, as demonstrated by the striking increase in the FUCO:Chl ratio (Fig. 7c), iron addition enabled diatoms to grow despite a potentially limiting silicic acid availability. Although laboratory studies have shown that the dominant PSC in iron-limited cultures of *Phaeocystis* is HEX and BUT while the dominant PSC in iron-replete *Phaeocystis* cultures is FUCO (van Leeuwe and Stefels, 1998; Schoemann et al., 2005), visual inspections of iron-enriched north patch samples confirmed a predominance of pennate diatoms (Brown et al., 2002; Jill Peloquin, pers. comm.). Very few *Phaeocystis* colonies were observed and those seen were small in size (Jill Peloquin, pers. comm.).

4.2.2. No iron-enrichment effect on the proportional composition of size fractions or phytoplankton pigments poleward of the SBACC south patch

Remarkably, iron enrichment in the south patch generated an increase in primary productivity without a concomitant shift of the proportional composition of size fractions and phytoplankton pigments. This result is unlike any other in situ iron-enrichment experiment reported to date (including the SOFeX north patch discussed above) where increases in productivity as a result of iron additions always co-varied with a shift in the phytoplankton assemblage from picoplankton to microplankton (Coale et al., 1996; Boyd et al., 2000; Gervais et al., 2002; Tsuda et al., 2003; Boyd et al., 2004). Tabulated results show an increase in the % $>20\,\mu m$ Chl from 50% to 58% (Table 2) consistent

with the de Baar et al. (2005) interpretation. However, as evidenced by the time series plots of % >20 μm Chl (Fig. 5b) and % diatom Chl_{HPLC} (Fig. 8b), both IN patch and ambient data are variable and quite similar to each other. Neither the IN nor the ambient % >20 μm Chl linear regressions versus day gave slopes that were significantly different from zero, which confirms the null hypothesis that there was no change in the % >20 μm Chl size fraction over the course of the experiment (Fig. 5b). Although the mean of the IN % diatom Chl_{HPLC} was higher than the mean OUT % diatom Chl_{HPLC}, the time series data show this difference was mainly a function of the one OUT observation late in the experiment and that one OUT observation was similar to some of the IN observations (Fig. 8b). Because there was little change to the composition of the phytoplankton assemblage, we conclude that the iron-induced increase in primary productivity was driven primarily by the improved physiology of the existing phytoplankton assemblage.

4.3. *Significance of fluorescent, non-photosynthetic chloropigments*

Significant concentrations of non-photosynthetic Chl derivatives have been reported for the Arabian Sea during the late SW monsoon when diatoms were abundant (Barber et al., 2001), in the Southern Ocean ACC during the SOIREE experiment (Gall et al., 2001), in Antarctic Polar Frontal Zone waters in late austral summer (Hiscock et al., 2003) and in the northeast Subarctic Pacific during summer (Suzuki et al., 2005). In the Arabian Sea, much of this non-photosynthetic fluorescence was attributed to the presence of chlorophyllide *a* (Barber et al., 2001). Gall et al., 2001 however, reported that chlorophyllide *a* was not responsible for a similar phenomenon observed during the SOIREE experiment but did not elaborate. Hiscock et al. (2003) corroborated that this discrepancy could not be attributed solely to chlorophyllide *a* and must be due to an unresolved factor affecting the fluorometric determinations. During the AESOPS Southern Ocean cruises the abundance of non-photosynthetic chloropigments increased as the growing season progressed, which may have reflected a time-related mechanism (i.e. senescence of ungrazed diatoms) as noted by Hiscock et al. (2003), a space-related mechanism, or both, because each consecutive AESOPS cruise progressed farther poleward as the ice edge retreated. Suzuki et al. (2005) reported this non-chlorophyllide *a* related discrepancy during the Subarctic Pacific iron enrichment (SEEDS) and concluded that the relationship between the fluorometric and HPLC measurements was "similar in timing and relative change" without specific reference to any iron addition effects.

As the SOFeX experiment progressed, one or more non-photosynthetic fluorescent compounds other than chlorophyllide *a* accumulated over the 27 d of observations in the iron-enriched surface ocean of the region poleward of the SBACC (Fig. 9b) where the proportion of diatoms in relation to the total Chl remained relatively unaffected by iron addition (Fig. 8b). Conversely, such compounds did not accumulate in the Subantarctic Zone where the phytoplankton assemblage transitioned from mostly picoplankton to a large component of diatoms over a period of 40 d. Thus, the simple presence or absence of diatoms does not correlate with the presence of this (these) as yet unidentified compound(s). Other factors, either in addition to or instead of the presence of senescing diatoms, are necessary to explain this phenomenon.

4.4. *Significance of iron enrichment to P^{B*}_{OPT} in the southern ocean, poleward of the SBACC*

In the ambient waters outside of the SOFeX south patch, the observed decline of hourly P^{B*}_{OPT} was driven by the increase of Chl concentrations while primary production remained at similar rates throughout the experiment. Iron enrichment in the south patch had two effects on photosynthetic performance: (1) it counteracted the decline of hourly P^{B*}_{OPT}, effectively extending the functional photosynthetic day length and (2) it enabled hourly P^{B*}_{OPT} to respond to daily PAR variability. Because the proportional composition of the iron-enriched south patch phytoplankton assemblage (based on size fractions and indicator pigments) remained comparable to that of the ambient assemblage, iron-differentiated P^{B*}_{OPT} reflected in situ changes in cell physiology rather than a response due to a compositional change in the phytoplankton assemblage present.

We note that primary productivity algorithms (Campbell et al., 2002; Carr et al., 2006) that employ P^{B}_{OPT} modeled from sea surface temperature (Behrenfeld and Falkowski, 1997) or mixed layer

depth (Johnson and Howd, 2000) in conjunction with remotely sensed Chl concentrations would underestimate productivity for the iron-enriched south patch SOFeX experiment because, while the temperature and mixed layer depth were the same for both ambient and iron-enriched waters, measured P^{B*}_{OPT} was higher in the iron-enriched patch than in ambient waters.

For the SOFeX south patch experiment phytoplankton biomass-specific primary productivity can be inferred to have increased on the order of 3-fold, based upon a ~5-fold increase in PP, a 5-fold increase in Chl^{*}_{HPLC} and a ~3-fold decrease POC:Chl^{*}_{HPLC} if the change in POC:Chl^{*}_{HPLC} was due solely to a change in phytoplankton carbon (see the discussion in Section 4.5).

4.5. Significance of iron enrichment to POC:Chl in the Southern Ocean poleward of the SBACC

There are two main factors that may influence the POC:Chl ratio, the first being an increase in Chl per unit of algal carbon (physiological response) and the second being an increase in algal associated carbon relative to heterotrophic carbon (POC composition). High POC:Chl ratios are commonly found in conditions where phytoplankton growth is limited and living heterotrophic carbon biomass and non-living detrital organic carbon particles fuel "microbial loop" carbon recycling processes. Low POC:Chl ratios are characteristic of phytoplankton bloom conditions, where phytoplankton cells are growing rapidly, outpacing the accumulation of heterotrophs and particulate detritus.

In the open ocean, away from allochthonous, refractory particle inputs, POC correlates well with phytoplankton carbon (C_{phyto}). In situ POC:Chl, therefore, tends to reflect the characteristic C_{phyto}:Chl of the representative functional groups that make up an assemblage in a given set of environmental variables because C_{phyto}:Chl differs inherently between species and between functional groups. For example, diatoms have a lower C_{phyto}:Chl than cyanobacteria (Falkowski and Raven, 1997). This linkage between functional group and C_{phyto}:Chl is demonstrated by the results of the IRONEX 2 iron-enrichment experiment in the eastern Equatorial Pacific: iron addition resulted in a decrease of C_{phyto}:Chl from ~150 under ambient conditions to ~70 at the peak of the iron-stimulated bloom as the phytoplankton assemblage shifted from being composed of predominantly small cyanobacteria to large diatoms (Landry et al., 2000b). In addition to the differences among C_{phyto}:Chl ratios of different functional groups, variations in response to iron limitation within a single species also occur (Sunda and Huntsman, 2004) so that both physiological and assemblage factors may influence this ratio simultaneously.

In the iron-enriched SOFeX south patch, while both Chl and POC increased, Chl increased at a faster rate than POC (Fig. 11a). The proportion of bacterial carbon biomass in the POC was small (about 4% in the iron-enriched patch and 7% outside the enriched area (Oliver et al., 2004)) and is negligible compared to the large changes in Chl and POC and therefore has little effect on POC:Chl. An increase in microzooplankton POC would act to increase the water column POC:Chl. The decrease seen in POC:Chl in response to iron enrichment in the south patch poleward of the SBACC (Fig. 11b) must be driven by C_{phyto}. This in situ observation is consistent with single species cultures in which slow-growing phytoplankton cells relieved of low light availability or low temperature stress (Geider, 1987), or iron limitation (Sunda and Huntsman, 2004), grew larger and had a lower C_{phyto}:Chl than resource limited, slow-growing phytoplankton. In the SOFeX south patch, POC:Chl decreased 3-fold in response to iron addition. Because the proportional composition of the phytoplankton assemblage was relatively unchanged by iron addition, this decrease in POC:Chl must have resulted from a change in phytoplankton physiology.

4.6. Diatom dominance poleward of the SBACC

Two points should be stressed regarding the proportional composition of the phytoplankton assemblages poleward of the SBACC relative to other HNLC regions. In the ambient waters in late summer, there were both (1) a greater proportion of diatoms than has been observed in other HNLC, low iron environments (e.g. ~50% in ambient south patch vs. ~>10% elsewhere, including SOFeX ambient north patch) and (2) a relatively low proportion of picoplankton compared to other HNLC environments (e.g. ~30% in ambient south patch vs. ~>70–80% elsewhere, including SOFeX ambient north patch). This uncommon compositional balance could be maintained either by conditions relatively favorable for diatoms, by conditions relatively unfavorable for picoplankton, or by a combination of both factors.

Dominance of diatoms is a consistently observed characteristic of the Southern Ocean poleward of the SBACC (Deacon, 1963) and may result from a series of conditions that differentially favor diatom growth and survival relative to other taxa. An early spring diatom bloom is likely facilitated by seasonal sea ice cover and subsequent melting due to a combination of optimal conditions: seasonal maximum nutrient and micronutrient concentrations (Sedwick and DiTullio, 1997; Hiscock et al., 2003); stratification (Smith et al., 2003); and perhaps diatom "seeding" (Gran, 1900; Garrison et al., 1987; Lizotte, 2001). Silicic acid concentrations well in excess of nitrate concentrations (Brzezinski et al., 2003; Sarmiento et al., 2004) may facilitate diatom productivity despite waning iron concentrations as the season progresses. An abbreviated polar growing season may not be long enough for picoplankton, with large surface-to-volume ratios, to exhibit their nutrient uptake advantage over larger diatoms. Grazing pressure may be reduced in the Southern Ocean because of low temperatures that may inhibit specific grazing rates (Huntley and Lopez, 1992; Clarke, 2003; Iguchi and Ikeda, 2005) and heavily silicified diatoms as prey, which would reduce assimilation efficiency and specific growth rates of grazers.

In previous iron-enrichment experiments, the "bloom" of the diatom population is explained by grazing rates that lag behind phytoplankton growth rates, whereas the lack of a picoplankton "bloom" is due to micrograzing rates that rapidly match picoplankton specific growth rates (Landry et al., 2000a; Barber and Hiscock, 2006). In the Southern Ocean poleward of the SBACC, micrograzing did not prevent the accumulation of picoplankton. Micrograzers may be slower to match the increased abundance of picoplankton in these cold waters than in temperate waters.

4.7. Seasonal context of primary productivity in the high latitude southern ocean

Primary productivity results of SOFeX and AESOPS (Figs. 2e and f) should be considered in a seasonal context with respect to light availability and ice cover (Comiso, 1999) (Fig. 12). In the north patch, iron enrichment allowed primary productivity to far exceed values measured in the same region during the AESOPS cruise earlier in the season (but different year) when irradiance was near maximal (Fig. 12a), supporting the hypothesis that primary productivity is iron-limited rather than PAR-limited in late summer in the Subantarctic Zone. No annual sea ice forms at the latitude of the north patch. In the south patch, iron enrichment took place near the middle of the short seasonal growing season with respect to daily PAR and open, ice-free water (Fig. 12b). Iron addition increased PP_{EU} despite waning daily PAR. No early season AESOPS data are available for comparison because those cruises did not extend to this region, which was ice covered in 1998. Poleward of the SBACC, as winter advances, light availability decreases to zero, seasonal ice cover increases to nearly 100%, and primary production will cease regardless of micronutrient concentration. The resulting 3- to 5-fold increase in daily PP_{EU} under iron-replete conditions (Table 2) is valid only for the brief portion of the dynamic season during which the south patch experiment was conducted. Annual productivity in an iron-replete Southern Ocean poleward of the SBACC would be much less than 3–5 times higher than annual present day productivity because of the limits imposed by seasonal ice coverage and polar darkness.

4.8. Seasonal implications of the SOFEX experiment poleward of the SBACC (south patch)

An iron-enrichment experiment in the high silicic acid waters poleward of the SBACC performed either earlier in the spring or later in the fall probably would have a different outcome from that of the SOFeX south patch experiment, which took place during the late summer. Specifically, in spring the south patch region would be exposed to increasing seasonal irradiance and stratification while surface waters would contain their annual maximum ambient iron and macronutrient concentrations. We hypothesize that because the region would be optically and biogeochemically primed to support a natural bloom, experimental iron enrichment would produce little or no biological response in the ambient phytoplankton. An iron addition experiment performed later in autumn, as solar irradiance rapidly diminishes, would give more insight into the role of iron in enhancing photosynthetic performance under low light, short photoperiod conditions. This enhancement, in effect, would expand the Antarctic growing season. The consequences of this potential expansion could be significant in terms of high latitude phenology of the food web (Edwards and Richardson, 2004) or

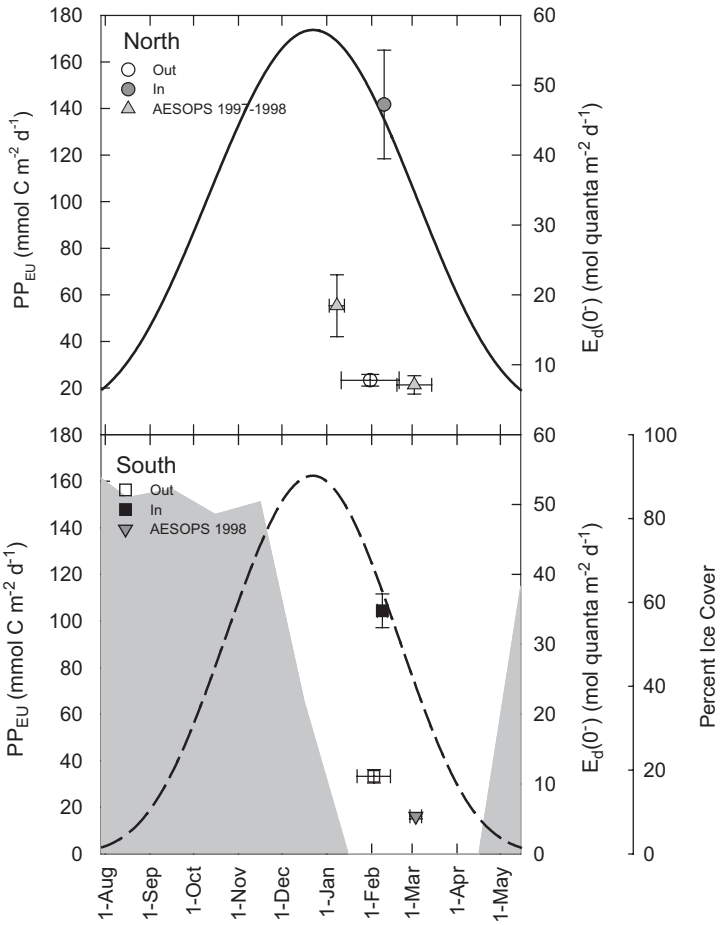

Fig. 12. Temporal relationship of primary productivity, irradiance and ice cover at the north and south patches. Solid and dashed lines are daily irradiance values for 56°S latitude (north patch) and 66°S latitude (south patch), respectively. Gray shading is percent monthly mean ice cover for the winter of 2001–2002 [data courtesy of the National Snow and Ice Data Center; (Comiso, 1999)] for the south patch, poleward of the SBACC. Seasonal ice does not extend to the Subantarctic Zone north patch. Symbols represent primary productivity and median day. OUT PP_{EU} is the mean of all OUT stations. IN PP_{EU} values are means of three maximum IN "full" stations as described for Tables 1 and 2. Vertical error bars represent standard error of mean productivity. Horizontal error bars represent day ranges.

biogeochemical partitioning of carbon (Buesseler et al., 2003).

5. Summary

Primary productivity and Chl: Iron enrichment of the cold, low silicic acid north patch waters of the Subantarctic Zone at about 56°S and of the very cold, high silicic acid south patch region poleward of the SBACC at about 66°S increased total productivity and Chl biomass by 5-fold or more at both sites. Productivity and Chl biomass increased in all size fractions. Total productivity and Chl biomass responses to iron addition were remarkably similar in these two dissimilar habitats.

Size composition: Iron enrichment differentially affected the size-fraction proportions of the phytoplankton assemblages at the north and south patch sites. The proportion of the microplankton size fraction increased greatly in the low silicic acid north patch waters but was virtually unchanged by iron addition in the high silicic acid south patch waters where large microplankton were responsible for about 50% of total productivity both before and after iron enrichment.

Pigment composition: In parallel with the size-fraction response, iron enrichment differentially affected the phytoplankton assemblage composition of the two sites. Despite the low silicic acid concentration in the north patch waters, diatoms (as determined from indicator pigments) greatly

increased in both absolute and relative abundance. In the high silicic acid south patch, the initial assemblage was about half diatoms and iron addition did not affect this proportional diatom component notwithstanding a large absolute increase in diatom abundance.

Non-photosynthetic chloropigments: Unidentified, non-photosynthetic but fluorescent chloropigments were present in ambient waters and accumulated to about 2-fold that of the ambient concentrations in the iron-enriched, high silicic acid south patch waters as the bloom developed. This unidentified fluorescence was not observed in the low silicic acid north patch in either ambient waters or the iron-enriched patch.

Photosynthetic performance: At the high silicic acid south patch site the ambient hourly photosynthetic performance (P^{B*}_{OPT}) decreased as a function of decreasing daily photoperiod at 66°S. Iron addition significantly reduced this seasonal decrease in photosynthetic performance, in effect lengthening the functional growing season and enabling photosynthetic performance to respond to daily available PAR.

Carbon to Chl ratio: In the high silicic acid south patch waters the initial POC to Chl ratio was high (~300:1) but decreased in response to iron addition to 100:1. Because the proportional taxonomic composition did not change, the change in this ratio represents primarily a physiological response, rather than a shift in the phytoplankton assemblage.

Significance of iron enrichment: Despite a potential 3- to 5-fold increase in primary productivity (PP_{EU}) under iron-replete conditions in late summer, the effect of iron on annual productivity in the Southern Ocean poleward of the SBACC is limited by seasonal ice coverage and the dark of polar winter.

Acknowledgments

Two anonymous reviewers provided careful and thoughtful comments which greatly improved this paper. We thank the captains and crews of the R/V *Roger Revelle*, the R/V *Melville* and the USCGS *Polar Star*. This SOFeX mission would not have been possible without the efforts of project leader Kenneth Coale, co-chief scientists Ken Johnson and Ken Buesseler, and the entire SOFeX science team. Shipboard assistance from Jill Peloquin, Liza Delizo, Sara Jane Tanner and Amy Apprill is greatly appreciated. Mark Altabet, Burke Hales, William Hiscock, Craig Hunter, Jill Peloquin and David Timothy provided data. We owe special gratitude to Craig Neill for sharing his electronics expertize aboard the R/V *Revelle*. Support for this research was provided by the Division of Ocean Sciences and the Office of Polar Programs at the US National Science Foundation (NSF Grants: OCE-9911441 to RTB, OCE-9912230 to RRB, OPP-0000329 to WOS). VPL and DAS were supported in part by OCE-0000329 awarded to Francisco Chavez of Monterey Bay Aquarium Research Institute. This is VIMS contribution number 2817.

References

Altabet, M.A., Francois, R., 2001. Nitrogen isotope biogeochemistry of the Antarctic Polar Frontal Zone at 170 degrees W. Deep-Sea Research Part II—Topical Studies in Oceanography 48, 4247–4273.

Barber, R.T., Hiscock, M.R., 2006. A rising tide lifts all phytoplankton: growth response of other phytoplankton taxa in diatom-dominated blooms. Global Biogeochemical Cycles 20 GB4S03, doi:10.1029/2006GB002726.

Barber, R.T., Sanderson, M.P., Lindley, S.T., Chai, F., Newton, J., Trees, C.C., Foley, D.G., Chavez, F.P., 1996. Primary productivity and its regulation in the equatorial Pacific during and following the 1991–1992 El Nino. Deep-Sea Research Part II—Topical Studies in Oceanography 43, 933–969.

Barber, R.T., Borden, L., Johnson, Z., Marra, J., Knudson, C., Trees, C.C., 1997. Ground truthing modeled k-PAR and on-deck primary productivity incubations with in situ observations. Society of Photo-Optical Instrumentation Engineers 2963, 834–839.

Barber, R.T., Marra, J., Bidigare, R.C., Codispoti, L.A., Halpern, D., Johnson, Z., Latasa, M., Goericke, R., Smith, S.L., 2001. Primary productivity and its regulation in the Arabian Sea during 1995. Deep-Sea Research Part II—Topical Studies in Oceanography 48, 1127–1172.

Behrenfeld, M.J., Falkowski, P.G., 1997. Photosynthetic rates derived from satellite-based chlorophyll concentration. Limnology and Oceanography 42, 1–20.

Bidigare, R.R., Van Heukelem, L., Trees, C.C., 2004. Analysis of algal pigments by high-performance liquid chromatography. In: Andersen, R.A. (Ed.), Culturing Methods and Growth Measurements. Academic Press, New York, pp. 327–342.

Boyd, P.W., Watson, A.J., Law, C.S., Abraham, E.R., Trull, T., Murdoch, R., Bakker, D.C.E., Bowie, A.R., Buesseler, K.O., Chang, H., Charette, M., Croot, P., Downing, K., Frew, R., Gall, M., Hadfield, M., Hall, J., Harvey, M., Jameson, G., LaRoche, J., Liddicoat, M., Ling, R., Maldonado, M.T., McKay, R.M., Nodder, S., Pickmere, S., Pridmore, R., Rintoul, S., Safi, K., Sutton, P., Strzepek, R., Tanneberger, K., Turner, S., Waite, A., Zeldis, J., 2000. A mesoscale phytoplankton bloom in the polar Southern Ocean stimulated by iron fertilization. Nature 407, 695–702.

Boyd, P.W., Law, C.S., Wong, C.S., Nojiri, Y., Tsuda, A., Levasseur, M., Takeda, S., Rivkin, R., Harrison, P.J., Strzepek, R., Gower, J., McKay, R.M., Abraham, E.,

Arychuk, M., Barwell-Clarke, J., Crawford, W., Crawford, D., Hale, M., Harada, K., Johnson, K., Kiyosawa, H., Kudo, I., Marchetti, A., Miller, W., Needoba, J., Nishioka, J., Ogawa, H., Page, J., Robert, M., Saito, H., Sastri, A., Sherry, N., Soutar, T., Sutherland, N., Taira, Y., Whitney, F., Wong, S.K.E., Yoshimura, T., 2004. The decline and fate of an iron-induced subarctic phytoplankton bloom. Nature 428, 549–553.

Boyd, P.W., Jickells, T., Law, C.S., Blain, S., Boyle, E.A., Buesseler, K.O., Coale, K.H., Cullen, J.J., de Baar, H.J.W., Follows, M., Harvey, M., Lancelot, C., Levasseur, M., Owens, N.P.J., Pollard, R., Rivkin, R.B., Sarmiento, J., Schoemann, V., Smetacek, V., Takeda, S., Tsuda, A., Turner, S., Watson, A.J., 2007. Mesoscale iron enrichment experiments 1993–2005: synthesis and future directions. Science 315, 612–617.

Bracher, A.U., Tilzer, M.M., 2001. Underwater light field and phytoplankton absorbance in different surface water masses of the Atlantic sector of the Southern Ocean. Polar Biology 24, 687–696.

Brown, S.L., Landry, M.R., Selph, K.E., Bidigare, R.R., Christensen, S., Twining, B.S., Cassar, N., Johnson, Z., Sheridan, C., 2002. Plankton community response to iron-fertilization in the "Northern Patch" at 56°S. In: American Geophysical Union Fall Meeting, San Francisco, CA, USA.

Brzezinski, M.A., Dickson, M.L., Nelson, D.M., Sambrotto, R., 2003. Ratios of Si, C and N uptake by microplankton in the Southern Ocean. Deep-Sea Research Part II—Topical Studies in Oceanography 50, 619–633.

Buesseler, K.O., Barber, R.T., Dickson, M.L., Hiscock, M.R., Moore, J.K., Sambrotto, R., 2003. The effect of marginal ice-edge dynamics on production and export in the Southern Ocean along 170 degrees W. Deep-Sea Research Part II—Topical Studies in Oceanography 50, 579–603.

Campbell, J., Antoine, D., Armstrong, R., Arrigo, K., Balch, W., Barber, R., Behrenfeld, M., Bidigare, R., Bishop, J., Carr, M.E., Esaias, W., Falkowski, P., Hoepffner, N., Iverson, R., Kiefer, D., Lohrenz, S., Marra, J., Morel, A., Ryan, J., Vedernikov, V., Waters, K., Yentsch, C., Yoder, J., 2002. Comparison of algorithms for estimating ocean primary production from surface chlorophyll, temperature, and irradiance. Global Biogeochemical Cycles 16 (3), doi:10.1029/2001GB001444.

Carr, M-E., Friedrichs, M.A.M., Schmeltz, M., Aita, M.N., Antoine, D., Arrigo, K.R., Asanuma, I., Aumont, O., Barber, R., Behrenfeld, M., Bidigare, R., Buitenhuis, E.T., Campbell, J., Ciotti, A., Dierssen, H., Dowell, M., Dunne, J., Esaias, W., Gentili, B., Gregg, W., Groom, S., Hoepffner, N., Ishizaka, J., Kameda, T., Le Quere, C., Lohrenz, S., Marra, J., Melin, F., Moore, K., Morel, A., Reddy, T.E., Ryan, J., Scardi, M., Smyth, T., Turpie, K., Tilstone, G., Waters, K., Yamanaka, Y., 2006. A comparison of global estimates of marine primary production from ocean color. Deep-Sea Research II—Topical Studies in Oceanography 53, 741–770.

Clarke, A., 2003. Costs and consequences of evolutionary temperature adaptation. Trends in Ecology and Evolution 18, 573–581.

Coale, K.H., Johnson, K.S., Fitzwater, S.E., Gordon, R.M., Tanner, S., Chavez, F.P., Ferioli, L., Sakamoto, C., Rogers, P., Millero, F., Steinberg, P., Nightingale, P., Cooper, D., Cochlan, W.P., Landry, M.R., Constantinou, J., Rollwagen, G., Trasvina, A., Kudela, R., 1996. A massive phytoplankton bloom induced by an ecosystem-scale iron fertilization experiment in the equatorial Pacific Ocean. Nature 383, 495–501.

Coale, K.H., Johnson, K.S., Chavez, F.P., Buesseler, K.O., Barber, R.T., Brzezinski, M.A., Cochlan, W.P., Millero, F.J., Falkowski, P.G., Bauer, J.E., Wanninkhof, R.H., Kudela, R.M., Altabet, M.A., Hales, B.E., Takahashi, T., Landry, M.R., Bidigare, R.R., Wang, X.J., Chase, Z., Strutton, P.G., Friederich, G.E., Gorbunov, M.Y., Lance, V.P., Hilting, A.K., Hiscock, M.R., Demarest, M., Hiscock, W.T., Sullivan, K.F., Tanner, S.J., Gordon, R.M., Hunter, C.N., Elrod, V.A., Fitzwater, S.E., Jones, J.L., Tozzi, S., Koblizek, M., Roberts, A.E., Herndon, J., Brewster, J., Ladizinsky, N., Smith, G., Cooper, D., Timothy, D., Brown, S.L., Selph, K.E., Sheridan, C.C., Twining, B.S., Johnson, Z.I., 2004. Southern ocean iron enrichment experiment: carbon cycling in high- and low-Si waters. Science 304, 408–414.

Comiso, J., 1999. DMSP SSM/I montly mean polar gridded sea ice concentrations, July 2001–May 2002. In: Maslanik, J., Stroeve, J. (Eds.), National Snow and Ice Data Center, Boulder, CO.

de Baar, H.J.W., Boyd, P.W., Coale, K.H., Landry, M.R., Tsuda, A.P.A., Bakker, D.C.E., Bozec, Y., Barber, R.T., Brzezinski, M.A., Buesseler, K.O., Boye, M., Croot, P.L., Gervais, F., Gorbunov, M.Y., Harrison, P.J., Hiscock, W.T., Laan, P., Lancelot, C., Law, C.S., Levasseur, M., Marchetti, A., Millero, F.J., Nishioka, J., Nojiri, Y., van Oijen, T., Riebesell, U., A., R.M.J., Saito, H., Takeda, S., Timmermans, K.R., Veldhuis, M.J.W., 2005. Synthesis of 8 iron fertilization experiments: from the Iron Age in the age of enlightenment. Journal of Geophysical Research 110, doi:10.1029/2004JC002601.

Deacon, G.E.R., 1963. The Southern Ocean. In: Hill, M.N. (Ed.), The Sea. Wiley, New York, pp. 281–296.

Dugdale, R.C., Wilkerson, F.P., Minas, H.J., 1995. The role of a silicate pump in driving new production. Deep-Sea Research Part I—Oceanographic Research Papers 42, 697–719.

Edwards, M., Richardson, A.J., 2004. Impact of climate change on marine pelagic phenology and trophic mismatch. Nature 430, 881–884.

Falkowski, P.G., Raven, J.A., 1997. Aquatic Photosynthesis. Blackwell Science, Oxford, pp. 375.

Fitzwater, S.E., Knauer, G.A., Martin, J.H., 1982. Metal contamination and its effect on primary production measurements. Limnology and Oceanography 27, 544–551.

Franck, V.M., Bruland, K.W., Hutchins, D.A., Brzezinski, M.A., 2003. Iron and zinc effects on silicic acid and nitrate uptake kinetics in three high-nutrient, low-chlorophyll (HNLC) regions. Marine Ecology—Progress Series 252, 15–33.

Gall, M.P., Boyd, P.W., Hall, J., Safi, K.A., Chang, H., 2001. Phytoplankton processes. Part 1: community structure during the Southern Ocean Iron RElease Experiment (SOIREE). Deep-Sea Research Part II—Topical Studies in Oceanography 48, 2551–2570.

Garrison, D.L., Buck, K.R., Fryxell, G.A., 1987. Algal assemblages in Antarctic pack ice and in ice-edge plankton. Journal of Phycology 23, 564–572.

Geider, R.J., 1987. Light and temperature-dependence of the carbon to chlorophyll-a ratio in microalgae and cyanobacter-

ia—implications for physiology and growth of phytoplankton. New Phytologist 106, 1–34.

Gervais, F., Riebesell, U., Gorbunov, M.Y., 2002. Changes in primary productivity and chlorophyll *a* in response to iron fertilization in the Southern Polar Frontal Zone. Limnology and Oceanography 47, 1324–1335.

Gran, H.H., 1900. XI. Diatomaceae from the ice-floes and plankton of the arctic ocean. In: Nansen, F. (Ed.), The Norwegian North Polar expedition, 1893–1896: Scientific results. The Fridtjof Nansen Fund for the Advancement of Science, Christiania, Oslo, p. 73.

Hiscock, W.T., Millero, F.J., 2005. Nutrient and carbon parameters during the Southern Ocean iron experiment (SOFeX). Deep-Sea Research Part I—Oceanographic Research Papers 52, 2086–2108.

Hiscock, M.R., Marra, J., Smith, W.O., Goericke, R., Measures, C., Vink, S., Olson, R.J., Sosik, H.M., Barber, R.T., 2003. Primary productivity and its regulation in the Pacific Sector of the Southern Ocean. Deep-Sea Research Part II—Topical Studies in Oceanography 50, 533–558.

Huntley, M.E., Lopez, M.D.G., 1992. Temperature-dependent production of marine copepods—a global synthesis. American Naturalist 140, 201–242.

Hutchins, D.A., Sedwick, P.N., DiTullio, G.R., Boyd, P.W., Queguiner, B., Griffiths, F.B., Crossley, C., 2001. Control of phytoplankton growth by iron and silicic acid availability in the subantarctic Southern Ocean: experimental results from the SAZ Project. Journal of Geophysical Research-Oceans 106, 31559–31572.

Iguchi, N., Ikeda, T., 2005. Effects of temperature on metabolism, growth and growth efficiency of *Thysanoessa longipes* (Crustacea: Euphausiacea) in the Japan Sea. Journal of Plankton Research 27, 1–10.

Johnson, Z., Howd, P., 2000. Marine photosynthetic performance forcing and periodicity for the Bermuda Atlantic Time Series, 1989–1995. Deep-Sea Research Part I—Oceanographic Research Papers 47, 1485–1512.

Kadar, S., Leinen, M., Murray, J. (Eds.), 1993. US Joint Global Ocean Flux Study. Equatorial Pacific Protocols.

Kirk, J.T.O. (Ed.), 1994. Light and Photosynthesis in Aquatic Ecosystems. Cambridge University Press, New York.

Landry, M.R., Constantinou, J., Latasa, M., Brown, S.L., Bidigare, R.R., Ondrusek, M.E., 2000a. Biological response to iron fertilization in the eastern equatorial Pacific (IronEx II). III. Dynamics of phytoplankton growth and microzooplankton grazing. Marine Ecology—Progress Series 201, 57–72.

Landry, M.R., Ondrusek, M.E., Tanner, S.J., Brown, S.L., Constantinou, J., Bidigare, R.R., Coale, K.H., Fitzwater, S., 2000b. Biological response to iron fertilization in the eastern equatorial Pacific (IronEx II). I. Microplankton community abundances and biomass. Marine Ecology—Progress Series 201, 27–42.

Letelier, R.M., Bidigare, R.R., Hebel, D.V., Ondrusek, M., Winn, C.D., Karl, D.M., 1993. Temporal variability of phytoplankton community structure based on pigment analysis. Limnology and Oceanography 38, 1420–1437.

Lizotte, M.P., 2001. The contributions of sea ice algae to Antarctic marine primary production. American Zoologist 41, 57–73.

Martin, J.H., 1990. Glacial–interglatial CO_2 change: the iron hypothesis. Paleoceanography 5, 1–13.

Moore, J.K., Abbott, M.R., Richman, J.G., Nelson, D.M., 2000. The Southern Ocean at the last glacial maximum: a strong sink for atmospheric carbon dioxide. Global Biogeochemical Cycles 14, 455–475.

Morel, A., 1988. Optical modeling of the upper ocean in relation to its biogenous matter content (Case-I waters). Journal of Geophysical Research—Oceans 93, 10749–10768.

Morel, A., Maritorena, S., 2001. Bio-optical properties of oceanic waters: a reappraisal. Journal of Geophysical Research—Oceans 106, 7163–7180.

Nelson, D.M., Brzezinski, M.A., Sigmon, D.E., Franck, V.M., 2001. A seasonal progression of Si limitation in the Pacific sector of the Southern Ocean. Deep-Sea Research Part II—Topical Studies in Oceanography 48, 3973–3995.

Oliver, J.L., Barber, R.T., Smith, W.O., Ducklow, H.W., 2004. The heterotrophic bacterial response during the Southern Ocean Iron Experiment (SOFeX). Limnology and Oceanography 49, 2129–2140.

Orsi, A.H., Whitworth, T., Nowlin, W.D., 1995. On the meridional extent and fronts of the Antarctic Circumpolar Current. Deep-Sea Research Part I—Oceanographic Research Papers 42, 641–673.

Sarmiento, J.L., Gruber, N., Brzezinski, M.A., Dunne, J.P., 2004. High-latitude controls of thermocline nutrients and low latitude biological productivity. Nature 427, 56–60.

Schlitzer, R., 2003. Ocean Data View.

Schoemann, V., Becquevort, S., Stefels, J., Rousseau, W., Lancelot, C., 2005. *Phaeocystis* blooms in the global ocean and their controlling mechanisms: a review. Journal of Sea Research 53, 43–66.

Sedwick, P.N., DiTullio, G.R., 1997. Regulation of algal blooms in Antarctic shelf waters by the release of iron from melting sea ice. Geophysical Research Letters 24, 2515–2518.

Sigman, D.M., Boyle, E.A., 2000. Glacial/interglacial variations in atmospheric carbon dioxide. Nature 407, 859–869.

Smetacek, V.S., 1985. Role of sinking in diatom life-history cycles—ecological, evolutionary and geological significance. Marine Biology 84, 239–251.

Smith, W.O., Dinniman, M.S., Klinck, J.M., Hofmann, E., 2003. Biogeochemical climatologies in the Ross Sea, Antarctica: seasonal patterns of nutrients and biomass. Deep-Sea Research Part II—Topical Studies in Oceanography 50, 3083–3101.

Sunda, W.G., Huntsman, S.A., 2004. Relationships among photoperiod, carbon fixation, growth, chlorophyll a, and cellular iron and zinc in a coastal diatom. Limnology and Oceanography 49, 1742–1753.

Suzuki, K., Hinuma, A., Saito, H., Kiyosawa, H., Liu, H.B., Saino, T., Tsuda, A., 2005. Responses of phytoplankton and heterotrophic bacteria in the northwest subarctic Pacific to in situ iron fertilization as estimated by HPLC pigment analysis and flow cytometry. Progress in Oceanography 64, 167–187.

Takeda, S., 1998. Influence of iron availability on nutrient consumption ratio of diatoms in oceanic waters. Nature 393, 774–777.

Tsuda, A., Takeda, S., Saito, H., Nishioka, J., Nojiri, Y., Kudo, I., Kiyosawa, H., Shiomoto, A., Imai, K., Ono, T., Shimamoto, A., Tsumune, D., Yoshimura, T., Aono, T., Hinuma, A., Kinugasa, M., Suzuki, K., Sohrin, Y., Noiri, Y., Tani, H., Deguchi, Y., Tsurushima, N., Ogawa, H., Fukami, K.,

Kuma, K., Saino, T., 2003. A mesoscale iron enrichment in the western Subarctic Pacific induces a large centric diatom bloom. Science 300, 958–961.

van Leeuwe, M.A., Stefels, J., 1998. Effects of iron and light stress on the biochemical composition of Antarctic *Phaeocystis* sp. (Prymnesiophyceae). II. Pigment composition. Journal of Phycology 34, 496–503.

Wanninkhof, R., Sullivan, K.S., Top, Z., 2004. Air–sea gas transfer in the Southern Ocean. Journal of Geophysical Research 109, C08S19, doi:10.1029/2003JC001767.